ARMY RESEARCH LABORATORY

Modeling Indirect Vision Driving With Fixed Flat Panel Displays: Task Performance and Mental Workload

Christopher C. Smyth

ARL-TR-2701 MAY 2002

The findings in this report are not to be construed as an official Department of the Army position unless so designated by other authorized documents.

Citation of manufacturer's or trade names does not constitute an official endorsement or approval of the use thereof.

Destroy this report when it is no longer needed. Do not return it to the originator.

Army Research Laboratory
Aberdeen Proving Ground, MD 21005-5425

ARL-TR-2701 May 2002

Modeling Indirect Vision Driving With Fixed Flat Panel Displays: Task Performance and Mental Workload

Christopher C. Smyth
Human Research & Engineering Directorate

Abstract

The relation between mental workload and situational awareness and the effects on vehicle performance are of interest to designers of future combat ground vehicles. In this report, a micro-state task time line analysis of attention workload is used to describe a model of driving performance and mental workload for indirect vision driving. The model is based on the results of a field study in which a military vehicle was driven with flat panel, liquid crystal displays fixed in the cab and a forward viewing monocular camera array mounted on the front roof. The task load times for the model are calculated with a mathematical equation for vehicle speed as a function of the camera field of view. The vehicle speed equation is derived with consideration given to the effects of scene compression on the informational needs of the driver in a self-paced task. An analysis shows that the task performance and mental workload are separable for the short course runs used in the field study. The effect of indirect vision driving on mental workload is determined from the subjective ratings of perceived task loading that were reported in the field study. Along with the perceived workload, the study participants rated the mental measures of task allocated attention, situational awareness, motion sickness, and subjective stress. Because of collinearity, the perceived workload is regressed on the factorial components of a cognitive loading space derived from a factorial analysis of the mental measures. Following rotation to a "skills-rules-knowledge" cognitive processing space derived from the clustering of the measures, the perceived workload is shown to be a function of the skills and rule-based components. On this basis, a micro-state time line model is proposed for the task information processing. In addition to the attention allocated to the driving task, the model includes attention to cognitive maps for route navigation and the monitoring of the internal somatic state for motion sickness. The task loading measures generated by the model are compared to the reported values with significant results. Finally, the model results are used to construct information flow networks for task analysis workload simulation studies. The model is intended for future work in predicting fatigue and performance errors that are induced by mental workload during indirect vision driving.

ACKNOWLEDGMENTS

The author would like to express appreciation for the support and interest in this research by Mr. Bruce Brendle and Ms. Melissa J. Karjala of the U.S. Army Tank Automotive Development and Engineering Center at Warren, Michigan. Our thanks to Dr. Joseph Heimerl of the U.S. Army Research Laboratory (ARL) for his review and discussion of the mathematical derivations. The author would like to express appreciation for the support and interest in this study by Dr. Laurel Allender, Mr. John Lockett, Ms. Lucia Salvi, and Ms. Diane Mitchell, all of ARL, for their discussions of the Improved Performance Research Integration Tool simulation program concepts. The author would like to thank Linda Fatkin of ARL for her discussions of the relation between subjective stress and perceived workload. Again, the author would like to thank David Harrah and Christopher Stachowiak of ARL for their guidance and close scrutiny as to purpose and detail in the preparation of this report. Finally, in addition to the ARL reviewers including Mr. Troy Kelly, the author would like to thank Dr. Christopher D. Wickens of the University of Illinois and Ms. Susan Archer of Micro Analysis & Design, Inc., for their close review and extremely helpful critiques of this manuscript.

The authors further thank Nancy Nicholas of ARL for technically editing this document.

INTENTIONALLY LEFT BLANK

Contents

Figures

Tables

INTENTIONALLY LEFT BLANK

MODELING INDIRECT VISION DRIVING WITH FIXED FLAT PANEL DISPLAYS: TASK PERFORMANCE AND MENTAL WORKLOAD

1. Introduction

In this section of the report, we describe the background rationale for the model development as it pertains to indirect vision driving and the effects on task performance and mental workload. Of particular interest is the effect of indirect vision driving on the mental performance of the crew, the measures of this performance, the inclusion of these parameters in driving models, and the experimental basis for our development.

1.1 Background

The Army needs combat vehicles that are smaller, lighter, more lethal, survivable, and more mobile to support a rapidly deployable force. Combined with the need to assimilate and distribute more information to, from, and within the vehicle as the Army moves toward a digital battlefield, there is the need for an increase in vehicle and command, control, communications, computers, and intelligence systems integration and performance. Consequently, the Army will need sophisticated, highly integrated crew stations for these future combat vehicles. In support of future vehicle design, the U.S. Army Tank Automotive Research Development and Engineering Center (TARDEC) is developing the Crew Integration and Automation Test bed (CAT) Advanced Technology Demonstrator (ATD). The purpose of the CAT ATD is to demonstrate crew interfaces, automation, and the integration technologies required to operate and support future combat vehicles. In support of this effort, the Human Research and Engineering Directorate of the U.S. Army Research Laboratory (ARL) is providing human factors expertise in determining the effect of these new crew station technologies with a continuing series of studies and investigations. The results can dramatically increase the operating effectiveness and capabilities with fewer crew members, thereby contributing to smaller and lighter weapon systems.

1.2 Indirect Vision Systems

To satisfy the Army requirements, designers of future armored combat vehicles will place the crew stations deep within the hull of the vehicle. For protection against direct and indirect fire as well as chemical and biological agents, the crew will operate with their hatches closed and sealed. The conventional optics, consisting of periscopic vision blocks and optical sights, will be replaced by electronic displays at the crew stations and by external vehicle-mounted sensors. These indirect vision systems will most likely show computerized digital images that are captured from the camera arrays on the vehicle. The crew member will

see a selected portion of the computerized display buffer that depends on his or her role and viewing direction. The display design may use a set of panel-mounted displays, either cathode ray tube (CRT) or flat panel liquid crystal displays (LCD), which are fixed in a panoramic arrangement about the crew member's station. No doubt, future vision systems will appear to the user as "see-through armor," by incorporating virtual reality components for the seemingly direct viewing of the external scene. However, because of the reduced resolution and physical isolation inherent to the technology, a question of interest to designers is the effect on mental processing and thus on task performance.

1.3 Workload and Situational Awareness

Human operators can perform well with less-than-optimal system designs by increasing their efforts to meet the more demanding workload. The problem is that over time, excessive workload can lead to fatigue and increased errors. Furthermore, the increased flow of information and tasks may result in a loss of situational awareness; this is because the ability of humans to process information is innately limited. As noted by Endsley (1995, 1993b), situational awareness is a precursor to optimal performance, since a loss in awareness impacts decision making and leads to a risk of performance error.

1.4 Motion Sickness

Another issue influencing task performance is the possibility of motion sickness, which can occur in an enclosed cab area with spatial disorientation. As noted by Yardley (1992), motion sickness is provoked by sensory conflict between the visual and sensorimotor activities that involve the vestibular system through head movements. Associated with motion sickness is a constellation of mainly autonomic symptoms such as pallor, drowsiness, salivation, sweating, nausea, and finally, vomiting in the more severe cases of sickness. Although some individuals may eventually adapt to situations that initially provoke sickness (Yardley, 1992; Baltzley, Kennedy, Berbaum, Lilienthal, & Gower, 1989), others do not, and the occurrences may be severe enough to arrest task performance until the symptoms subside.

1.5 Subjective Stress

Finally, another performance issue is the effect on the cognitive functioning of the emotional stress state of the operator. This is important because the commander in the two-person armored vehicle design may have the additional role of being the driver. The commander may be expected to cognitively process information acquired visually from data displays for decision making such as for target engagement and to select routes of approach from digital map displays. These cognitive functions may be composed of such basic elements as mathematical, semantic, logical, and spatial reasoning, as well as higher level functions such as planning. In addition, the ability and desire to acquire and process information may be influenced by the stress state of the commander.

1.6 Driving Models

The driving models in the literature are based on classical frequency control theory (Hess & Modjtahedzadeh, 1990) or the time-based modern control theory (Bekey, Burnham, & Seo, 1977). Developed to describe autonomous skill-based highway driving, the models use constant parameters to represent the human cognitive function of predictive preview and delay in neuromuscular response (Winsum & Godthelp, 1996; McAdams, 1988; Smiley, Reid, & Fraser, 1980). However, armored vehicle driving on a battlefield is a highly fluid situation with dynamically changing threats and objectives. In this case, the human cognitive functions involve the higher level processes (Rasmussen, 1983) to develop and apply rule-based schematics to guide and direct the skill-based behavior of driving. An essential element of this supervisory process is the development and maintenance of a mental model (Norman, 1988) of the driving task and the battlefield situation. For this reason, an appropriate model may be the skills-rules-knowledge (SRK) information processing model (Rasmussen, 1986, 1993) reformatted as a derivative of the human processor (Card, Moran, & Newell, 1983). In this model, inter-linked perceptual, cognitive, and motor processors operate on discrete micro-state events to represent human behavior. Further, the model should consider the allocation of attention resources and interference among processor channels to account for the limited capacity of human attention in task performance as described by the attention resource allocation model (Wickens, 1992). The superposition of executive cognitive processes by an expert system consisting of production rules (Kieras, Meyer, Mueller, & Seymour, 1998) supports the explicit declaration of rule-based reasoning appropriate for indirect vision driving. Finally, a realistic model will also include the effects of workload, situational awareness, motion sickness, and emotional stress on task performance.

1.7 Experimental Field Study

Before indirect vision systems can be designed for future military vehicles, materiel developers will need to know the potential impact of design parameters on combat performance. Because of this need, TARDEC asked ARL to conduct an experiment on the effects of indirect vision upon driving performance. In support of this request, ARL conducted a field study in the spring of 1999 of the ability of soldiers to drive a military vehicle with an external vehicle-mounted camera array and panel-mounted video displays. Further, we investigated the effects of indirect vision driving on the mental workload measures of attention allocation and perceived workload, situational awareness, induced motion sickness, subjective stress, and cognitive abilities. The results were compared to direct vision driving as representative of a "see-through armor" vision system. The experimental methodology and statistical results are reported in a separate report (Smyth, Gombash, & Burcham, 2001). This report describes the modeling development for task performance and mental workload that was derived from the results of the 1999 experiment.

2. Objective

A model of driving performance and mental workload is derived for indirect vision driving. The task times for the model are computed from a mathematical equation of vehicle speed as a function of the camera field of view (FOV). The effect of indirect vision driving on perceived mental workload is modeled with subjective measures of task allocated attention, situational awareness, motion sickness, and subjective stress that resulted from a field study. Following clustering relations among the measures, the perceived workload is regressed onto an SRK cognitive attention space derived for information processing. A micro-state activity model is proposed for the driving task, and the perceived workload and task attention measures are related to the time line activities of the model processors. The model results are used in task analysis workload simulation of indirect vision driving.

3. Field Experiment

In this section, we briefly review the experimental methodology, driving task, and experimental results upon which the analysis is based.

3.1 Experimental Methodology

For the indirect vision driving, three fixed flat panel, 640H x 480V pixel color LCDs were mounted side by side in the front of the cab of a high mobility multipurpose, wheeled vehicle. The displays received 30-Hz interlaced video returns via NTSC[1] (RS-170) to video graphic array signal converters, from a forward viewing monocular camera array that was mounted on the front roof of the vehicle and tilted slightly downward. The driver's seating position was enclosed to keep sunlight from "washing out" the displays and to eliminate the exterior view. The displays provided a panoramic 110° view of the camera video to the driver in the cab. Three different sets of camera lenses were used to provide near unity (150°), wide (205°), and extended (257°) camera FOVs. Unity FOV matches direct viewing in scene perspective. Eight military male volunteers served as participants in this study. They drove the experimental vehicle over a 590-meter driving course at Aberdeen Proving Ground, Maryland, which consists of S-curves, berms, and straight-aways, marked by 48 pairs of barrels. The experiment was within subjects with the three camera lenses and direct vision applied to the participants in a counterbalanced manner. In addition to recording course times and number of barrel strikes for data, subjective

[1] National Television System Committee

questionnaires for perceived workload, task allocated attention, situational awareness, motion sickness, and subjective stress, were applied to the participants at the end of each course run (Smyth, Gombash, & Burcham, 2001). These data are modeled in this report.

3.2 Driving Task of Experiment

The driving task performed by the participants is described in terms of the control activity. Figure 1 is a task analysis flow diagram for an experimental trial run. Following training, the driver had developed a strategy to maximize the course speed while minimizing the lane marker strikes. In this strategy, he used braking, steering, and acceleration to directly approach a pair of lane markers and then accelerate between them. The driver navigated the course by first finding the next marker pair from his mental map of the course and the display scene and then selecting an approach path that supported the driving strategy. He manually adjusted his course speed from the velocity flow field that he saw on the display scene. To do this, he (a) located the velocity field on the display, (b) evaluated the flow by comparing it to that learned in training, and (c) adjusted his speed and course by his manual control actions. As he neared the marker pair, he checked his orientation and manually steered to align the vehicle so that he could drive directly between the markers. This serial sequence of activities is reasonable, considering the time window available to the driver for approaching each marker pair, which was on the order of several seconds.

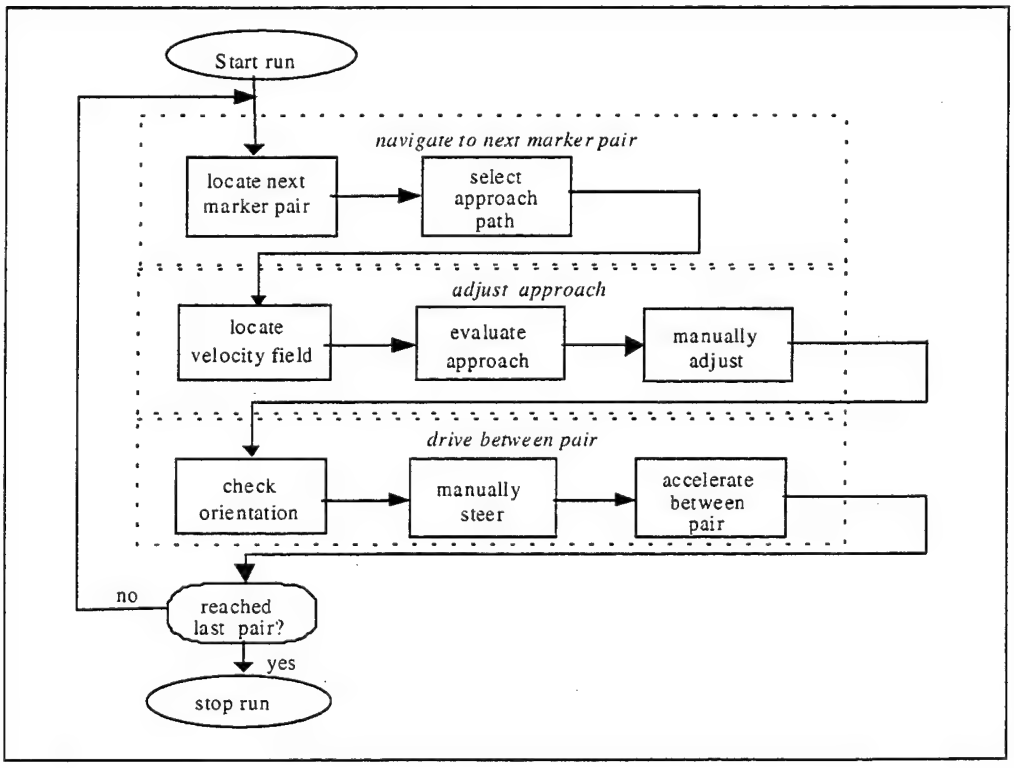

Figure 1. Task Analysis Flow Diagram for the Driving Task.

3.3 Summary of Experimental Results

For the relatively benign driving conditions (well marked course, good visibility, and essentially flat terrain), the participants successfully drove the vehicle with indirect vision for the different FOVs. However, with natural vision, they drove the course 25% faster and made 0.5% fewer lane marker strikes than they did with indirect camera systems. Furthermore, the course speed significantly decreased with increased camera FOV, while the number of lane markers increased slightly. While the course speed decreased with increased FOV, the speed of travel was perceived as increased because of the scene compression. Workload ratings show a significant increase in perceived workload with indirect vision, while an investigation of situational awareness shows an increase in the demand dimensions. While in the moving vehicle with the displays, most participants reported discomfort associated with motion sickness. The estimated subjective stress rating of the participants was least for natural vision and increased with indirect FOV.

3.4 Display Compression Ratio

The display compression ratio is a measure of the compression of the camera's scene by the display and is calculated as the ratio of the camera's horizontal FOV to that of the display's 110°. Here, the compression ratios for the near unity, wide, and extended camera FOVs are 1.364, 1.864, and 2.336, respectively. While the compression ratio is unity for direct viewing from the driver's seat in the vehicle, the scene has natural depth perception and resolution and free head movement over the entire viewing front. In contrast, the indirect viewing from the vehicle is limited to the panoramic displays with relatively limited resolution, no depth perception, and visual dead spaces between displays. There are also minor differences among the indirect vision displays such as the amount of hood and sky in the scene. For this reason, the direct and indirect vision systems were considered as different treatments for statistical analysis. However, much of the data variation in the experiment is explained by the display compression ratio, and for this reason, the ratio is used as a quantitative dimension in the following analysis of task load and speed performance.

4. Driving Speed Performance and Task Load

In this section, we show that the average course speed for the field study is predicted by a mathematical model developed for the vehicle speed as a function of the display compression ratio. The perceived speed of travel is discussed. In the derivation of the mathematical model, the information and decision execution time is assumed to remain constant across viewing conditions. The results show that the task performance and mental workload may be treated in separate analyses for the short course runs used in the field study. For this

reason, the task load times for the model are calculated independently of the mental workload analysis with a mathematical equation for vehicle speed as a function of the camera FOV.

4.1 Mathematical Model of Course Speed

A mathematical equation is derived that relates the speed of travel to the camera FOV for indirect vision driving. The driving task is self paced, with the speed adjusted to accommodate the information processing and reactive decisions that follow from the velocity flow field of the scene that appears on the display. The velocity flow field is generated by the apparent flow of terrain features across the display along the direction of travel. The decrease in scene resolution with display compression reduces the visibility of the terrain detail that provides the flow field. The display compression of the scene occurs with an increase in the camera FOV. With compression, the velocity flow appears to originate from a point in the scene that is closer to the front of the vehicle. Furthermore, the velocity flow appears faster than normal and to accelerate and move laterally as the vehicle moves forward because of scene distortion with compression (Smyth, Gombash, & Burcham, 2001). For this reason, the driver moves at a slower speed to allow time to evaluate course changes and execute motor responses. Also, the decrease in scene resolution with display compression increases the control-to-display-response ratio and thereby decreases the control sensitivity (Sanders & McCormich, 1993). The driver must make finer control adjustments with the compression in visual feedback to get the same control as with direct viewing. The driver reduces his or her driving speed to accommodate the rate of change in course variation and maintain a consistent error rate during the reduced control sensitivity.

Assuming self-paced driving with data limited by the velocity flow field on the display, a relation is derived between the vehicle speed of travel (υ) and the display compression ratio. See Figure 2 for the camera-to-scene geometry. Here, the compression ratio (α) is a measure of how much the display compresses the camera image return of the scene, and it is defined as the ratio of the camera's FOV to the display's FOV. Letting terrain features that define the velocity flow field on the display be fixed squares (linear dimension, δ), the apparent solid angular area (ω) of a feature as seen at an angle (θ) to the ground by the camera, is the ratio of the projected area divided by the square of the viewing distance (ρ) from the camera to the feature $\omega = (\delta/\rho)^2 * \sin(\theta)$. Fixing the camera on the vehicle at a height (η) above the ground, the apparent angular area is given by $\omega = (\delta/\eta)^2 * \sin^3(\theta)$, with the use of the sinusoidal relation between the camera height (η), viewing distance (ρ), and viewing angle (θ). To be noticed on the display, the apparent angular area of the feature must exceed a critical size (ω_c) determined by a psychophysical threshold value (ϖ) and the compression ratio(α), so that $\omega_\chi = \alpha * \varpi$. The viewing angle ($\theta_c$) corresponding to the critical size is given by

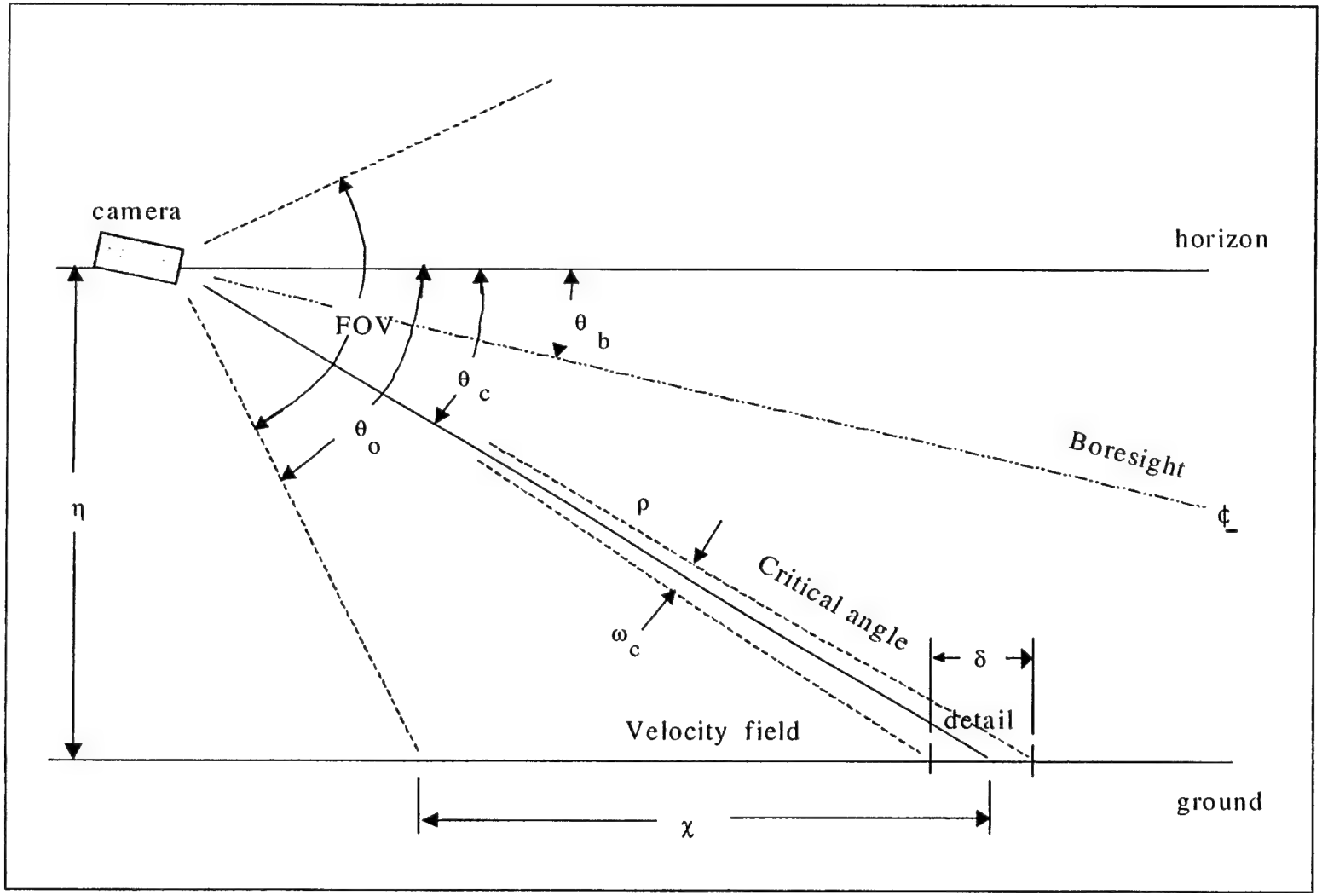

Figure 2. Camera Geometry.

$$\alpha * \varpi = (\delta/\eta)^2 * \sin^3(\theta_c), \quad (1)$$

since $\theta_c = \theta$, when $\omega = \omega_c$. The critical size determines the start of the velocity flow field on the display, since all flowing terrain features appear to originate from this level and then pass to the bottom of the screen and out of the camera's FOV.

For self-paced driving, the vehicle speed (υ) is given by the ratio of the length of travel (χ) along the ground corresponding to the flow field size, divided by an information processing and decision execution time (τ). Here, this processing time is assumed to be fixed by the task and the vehicle speed is given by $\upsilon = \chi/\tau$. Using the tangential relation between the ground distance and the viewing angle, the flow field ground length is

$$\chi = \eta * (\tan(\theta_o) - \tan(\theta_c))/(\tan(\theta_o) * \tan(\theta_c)). \quad (2)$$

This is true since the flow field is bound by the viewing angles for the critical sized features (θ_c) of the flow field and the bottom edge of the camera's view (θ_o), where $\theta_o = \theta_b + FOV/2$, as expressed in terms of the bore-sighting angle for the camera (θ_b) and the camera's vertical FOV. Note that since the camera's FOV is related to the display vertical field of view (FOV_d) by the compression ratio, the view angle for the bottom edge of the camera's view is $\theta_o = \theta_b + \alpha * FOV_d/2$. This expression can be reduced by assuming that the camera height is much less than the critical feature viewing distance and correspondingly, that the camera is boresighted toward the horizon. In this case, the tangent of the viewing angle is closely approximated by the sinusoidal value, and with the use of the sinusoidal expression for the critical viewing angle in terms of the threshold level, the expression for the vehicle speed reduces to

$$\upsilon = (\eta/\tau) * (\gamma * \alpha^{-1/3} - 1/\tan(\theta_b + \alpha * FOV_d/2)), \quad (3)$$

in which $\gamma = ((\delta/\eta)^2/\varpi)^{1/3}$, in terms of the display compression ratio. Note that the constant γ is on the order of 100, that is, $\gamma >> 1$, since the critical feature detail size (δ) is roughly on the order of a hundredth of the camera height (η), and the solid angle threshold (ϖ) is on the order of micro-steradians. The latter is true since the human visual acuity threshold is on the order of 1 visual second of arc. Further, the camera's FOV is quite large and with the boresight angle ($\theta_b = 13°$) and display vertical FOV ($FOV_d = 22.5°$) used in this study, the tangent of the lower boundary (θ_o) is greater than unity. With these assumptions, the second term in the expression for the vehicle speed may be ignored, and the equation reduces to $\upsilon = \kappa * \alpha^{-1/3}$ in which the equation constant is $\kappa = (1/\tau) * (\eta/\varpi)^{1/3} * (\delta)^{2/3}$. Assuming that the vehicle speed for unity display compression is equivalent to that for direct viewing (υ_1) and noting that this in turn is equal to the equation constant (κ), the vehicle speed for indirect viewing may be expressed as

$$\upsilon = \upsilon_1 * \alpha^{-1/3}, \tag{4}$$

in terms of the direct viewing speed and the display compression ratio.

The display compression of the scene image distorts the perception of the vehicle speed by the driver. Since a known object in the display scene will appear compressed in linear dimensions, it will appear perceptually at a greater range and will move toward the driver with a perceived speed (υ_p) greater than the actual speed (υ), according to $\upsilon_p = \alpha * \upsilon$. For this reason, even though the actual speed of data limiting performance for indirect view driving is less than that for direct viewing and decreases with display compression ratio, the perceived effect is the reverse. That is, the speed is perceived to be greater than that for direct viewing according to

$$\upsilon_p = \upsilon_1 * \alpha^{2/3}, \tag{5}$$

and to increase with compression ratio. Thus, although the drivers must travel at a slower speed to maintain control with increased display compression as compared to direct view driving, they perceive themselves to be traveling at a faster speed.

4.2 Driving Performance and Task Load

The course speed is shown to be predicted by the mathematical model developed for the speed as a function of the display compression ratio. The perceived speed of travel is discussed.

4.2.1 Course Speed

The predictive Equation (4) derived here is in the form of a product of the course speed times the display compression ratio (dcr) raised to 1/3 power with the product equal to a constant. Since the course times show statistically significant differences among treatments, the parameters of the equation are computed from these data with a regression analysis (adjusted-R square = 0.328, $p < .0004$, F = 16.136, df = 1, dfe = 30), resulting in

$$\text{speed (km/hr)} = 22.31 * \text{dcr}^{-0.332}. \tag{6}$$

The equation predicts that the average driving speed is greater for the direct vision and decreases with increasing camera FOV.

Figure 3 is a plot of the speed as a function of the display compression ratio. The figure shows a scatter plot for the experimental data, the mean data values, and the estimated regression line with 90% confidence intervals (CI) for the sample means. Considering the simplicity of the analysis, the close match between the predicted and average values is appealing. This is true, since the mean data values are within the 90% CI for all treatments except the near-unity FOV.

However, while the driver could see the vehicle hood with the other treatments, this was not true with the near-unity FOV since the hood was just below the camera's narrower view. Without the hood as a guide, the drivers presumably had to be more careful in controlling the vehicle's approach to the markers, and this may account for the slower than predicted speed. The point labeled "HMD study" was not part of the analysis and refers to a separate experiment conducted in 1996 with a helmet-mounted display used in place of the fixed display panels (Smyth & Whitaker, 1998). Of interest is that Equation (6) derived for the present experiment accurately predicts the mean speed for the 1996 study.

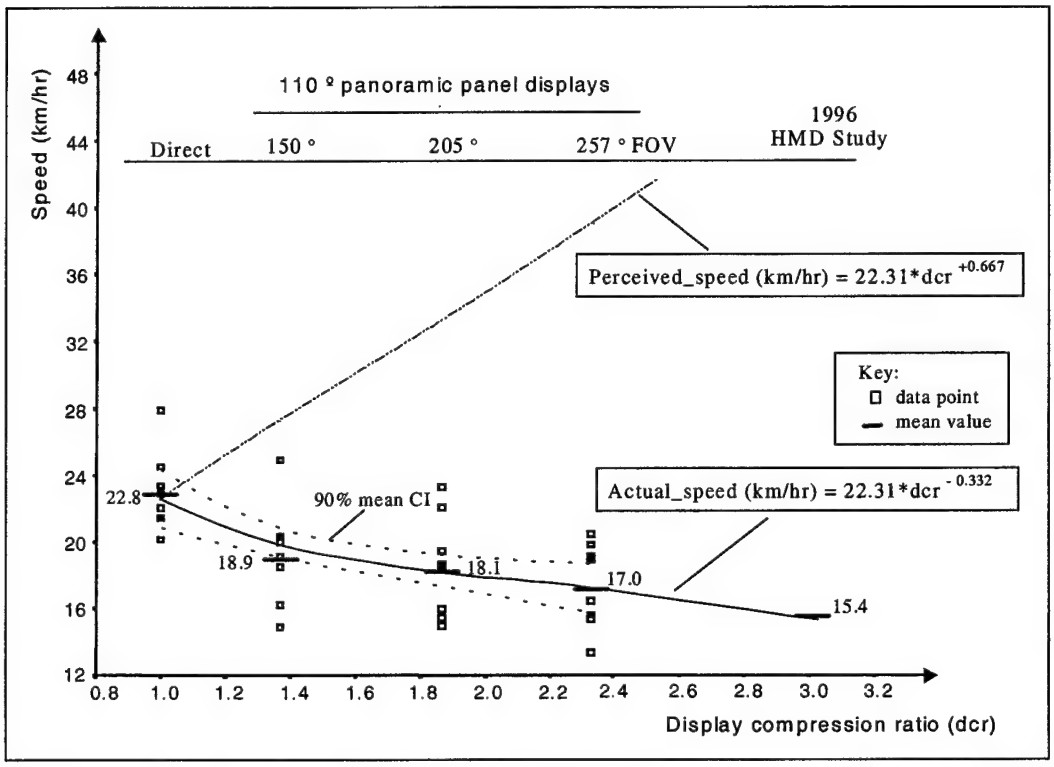

Figure 3. Course Speed as a Function of Display Compression Ratio.

4.2.2 Perceived Speed

For the indirect vision, the speed of travel according to Equation (5) is perceived to be greater than that for direct viewing and to increase with the compression ratio because of scene elongation. This effect is shown in Figure 3, where, although the predicted speed for indirect view driving is less than that for direct viewing and decreases with display compression ratio, the perceived speed is predicted to increase. Although no data were collected in the field study for the perceived speed, this effect agrees with the experiences reported by the study participants. Thus, although the drivers with indirect vision travel at a slower speed to maintain control with increased display compression, they may perceive themselves to be traveling at a faster speed in direct proportion to the compression ratio. For this reason, they may believe themselves to be traveling

faster than they actually are and may decelerate, resulting in a potential decrement in tactical performance.

4.3 Implications for Workload Simulation

The statistically significant match of the course speed equation to the field study data implies that the information and decision execution time may be assumed to remain constant across viewing conditions. This validates the assumption that the processor times remain constant, which is made in the micro models developed next to describe the mental workloads. The results suggest that the task load performance and mental workload may be treated separately in task workload analysis, at least for the short course runs used in the field study. In the two next sections, we develop a descriptive model of information processing and then apply the model to the driving task.

---

5. Information Processing Model

In this section, we describe an information processing model appropriate to the driving task. We start with task-directed behavior before describing model configuration, architecture, processor characteristics, and application to a driving model at the micro-state activity level.

5.1 Human Information Processing

The model is described from the level of task-directed behavior, which is composed of sequential behavior combined with performance assessment.

5.1.1 Task-Directed Behavior

Task-directed behavior is composed of hierarchical components: a sequential activity for task performance and an accompanying assessment activity used to maintain a mental model of the process. The mental model (Norman, 1988; Shepherd, 1978; Simon, 1987, 1957) contains a knowledge base understanding of the task and situational awareness. The task sequence consists of skill-level behavior, which is directed by a rule-based script type schema (Brookhuis, DeVries, & DeWaard, 1991) developed for the particular problem from the mental model. At the higher cognitive levels, an awareness of the surrounding problem structure is maintained to compose the schemas needed as new problems arise. As noted by Endsley (1993a, 1993b, 1996), this awareness can occur in the individual at several levels. These are (1) an awareness of the problem, (2) a knowledge of the problem class derived from pattern matching and the state of the elements comprising the problem structure for that class, and (3) an assessment of the consequences and a mapping of the problem and the elements to an appropriate solution scheme. Thus, situational awareness is determined by the knowledge of the operator and his or her understanding of the goals and tactical understanding (Selcon, Taylor, & Koritsas, 1991).

The maintenance of a mental model and the accompanying situational awareness is necessary for the continual planning of problem involvement, and this maintenance constitutes a form of secondary task with its own unique workload requirements. For this reason, problem solving is composed of dual tasks, which while competing for attention resources consists of a sequential activity focused on a particular problem and an accompanying maintenance of situational awareness of the problem environment. Performance is improved when the task demand is matched by the supply of knowledge and central processing resources in the human. The central processing may be conceived as drawing upon the cognitive resources according to the level of processing involved, that is, skill-level, rule-based, or knowledge-based behaviors (Rasmussen, 1983, 1986, 1993). Here, skill-based behavior provides the task performance, rule-based the governing schema for skill control, and knowledge-based the schema formation for the next task problem. Workload and awareness are related since attentional resources are used to acquire and maintain awareness. In turn, awareness of the task situation is needed for effective decision making and implementation. As with any task, awareness of the situation is limited by the attention capacity of the human (Wickens, 1992). The implication is that models of human information processing should include a component in memory which is specialized for situational awareness and a mental model of the task problem process (Gordon, 1997). The model should also include the attentional demands of complex decision making and problem solving, which are used to maintain situational awareness.

5.1.2 Model Description

The generic model of human information processing which is appropriate for driving follows the Norman-Shallice model (Shallice, Burgess, Schon, & Baxter, 1989). In this model, responses triggered by stimuli are modulated by a cognitive supervisor operating from an event contention scheduler through a database memory. A further refinement is Rasmussen's SRK model (1986, 1993) of cognitive control, with skill-, rule-, and knowledge-based behavior for task performance. At the rule-based level, stimuli act as cueing signals to activate automated sensory-motor patterns. Signs formed by feature formation from the cues activate associated stored rules following recognition at the rules level, and symbols result in planned decisions following identification at the knowledge level.

Following the theory of naturalistic decision making, the SRK model has been expanded into an information processing model (Gordon, 1997) with the use of recognition-primed decision making (Klein, Orasanu, Calderwood, & Zsambok, 1993; Zsambok & Klein, 1997). In this development, the cognitive levels of information processing are matched to Endsley's (1997) levels of situational assessment (SA). As with the SRK model, the skill-based processing is automatic with stimulus cues triggering an action response. In turn, the rule-based reasoning is intuitive and corresponds to Endsley's level 1 SA of cue integration.

At this level, the stimulus-cues trigger the retrieval of associated rules (cue-action "if-then" rules) from memory for the goal and action sequence to be executed. Knowledge-based reasoning is analytical and corresponds to Endsley's SA level 2 of diagnosis and planning, resulting in a decision for singular action and a plan of execution. With uncertainty and given sufficient time, more complex evaluation processes using analysis are employed with knowledge-based processing to plan solutions at Endsley's SA level 3 (Wickens, Gordon, & Liu, 1998).

A further refinement of rule-based reasoning is the executive-process interactive control (EPIC) model developed by Meyer and Kieras (1997a, 1997b). The model has been used for describing human performance at the level of concurrent perceptual motor and simple cognitive tasks. Meyer and Kieras argue that at a cognitive level, people apply distinct sets of production rules simultaneously for executing the procedures of multiple tasks. The capacity to process information at peripheral perceptual motor levels is limited. Flexible scheduling strategies are used to cope with such limits and to satisfy task priorities. These strategies are mediated by executive cognitive processes that adaptively coordinate concurrent tasks (Kieras, Meyer, Mueller, & Seymour, 1998). EPIC has been used to successfully simulate multiple task performance during a variety of laboratory circumstances.

Along these lines, Sanderson (1991) developed her "model human scheduler" which includes production rules for Rasmussen's (1986) skill-based, rule-based, and knowledge-based scheduling components, and the "model human processor" (Card, Moran, & Newell, 1983) to implement some cognitive steps (Sheridan, 1992).

5.1.3 Model Architecture

Following these developments, a schematic of a human information processing model that is suitable for a generalized driving task should include a processor for situational assessment decisions. In this generic model, the stimuli in the short-term store activate motor responses through the skill-based processor. Concurrently, a cognitive processor monitors the stimulus-triggered responses. Here, the cognitive processor is hierarchically divided into a rule-based processor and a knowledge-based processor. The rule-based processor controls the schema script used in the skilled responses and provides feedback of expectancy contentions to the knowledge-based processor through an attention supervisor. The feedback is generated during monitoring from discrepancies between the expected and the actual perceptions that are mapped into the trigger database. In response to contention, the knowledge-based processor schedules the rebuilding of the schema script used in rule-based reasoning. The working memory is the temporary storage for the rule- and knowledge-based activities, and all information flow between long-term memory and these processors passes through working memory including encoding of the perceptions (Baddeley,

1990, 1986, 1983). The long-term memory includes procedural production rules for schema scripts and a mental model of the task problem and situational awareness, which maps to the trigger database for associations. The attention supervisor controls the allocation of attention among the different functions.

5.1.4 Processor Characteristics

Following the Model Human Processor described by Card, Moran, and Newell (1983), the human behavior mechanics are represented by interlinked processors that perform the perceptual, cognitive, memory, and motor functions. The capabilities of the processors are specified by cycle times, decay periods, and capacity characteristics that are derived from psychophysical evidence. The perceptual processors pass receptor-transduced stimuli to short-term store areas in memory where they are encoded for further processing by working memory. As described by Card et al. (1983), working memory with time and capacity limitations consists of programs in the form of chunks that are "downloaded" from long-term memory. These programs are activated in the cognitive processor for rule-based decision making and the subsequent activation of the motor processors. The cognitive processor cycles through the program, modifying the contents of working memory according to their associations in long-term memory. Motor movements are executed as a sequence of discrete micro-movements with a feedback loop from the response to perception for correction. Rapid motor acts are executed in bursts of pre-programmed motor instructions following mental preparation.

5.1.5 Rule-Based Processor

Following Meyer and Kieras (1997a), the rule-based processor is an expert system with a production engine that interprets schematic script rules expressed as conditional action "if-then" statements. The processor cycles through a list of rules while testing for the status of the conditions, based on the input from the working memory, and executing (or "firing") the corresponding actions for those conditions that exist. The actions include modifications of the production rules and execution of appropriate motor processors. The model architecture interfaces the working memory with the rule interpreter within the cognitive processor. Further, the long-term memory has been expanded to include memory of production rules. In turn, the interpreter interfaces with the motor processors for the ocular, vocal, and manual functions through the skill-based processor. The visual processor has a direct input to the ocular motor processor for orienting responses to visual input. The design allows consideration of multiple tasks in parallel since the production rules may be formulated accordingly.

5.2 Processing Model for Driving

Figure 4 is a schematic of a driving model that incorporates the generic architecture for human information processing in the form of a digital process controller. The model of the human operator maps directly to the architecture of the information processing model with the autonomous skill-based control

mapping to the skill-based processor, the rule-based filtering and prediction control to the rule-based processor (i.e., rules interpreter), and the planning and supervisory control to the knowledge-based processor. The skill-based processor is the interface between the perceptual processors and the psychomotor processors. The working memory interfaces with the cognitive processors to the perceptual processor through the encoder, and to the long-term memory with the mental model and associated production rules. With input from the mental model and the skill-based processor, the trigger database is essential to the expectancy contention loop controlled by the rule-based processor with feedback to the attention supervisor.

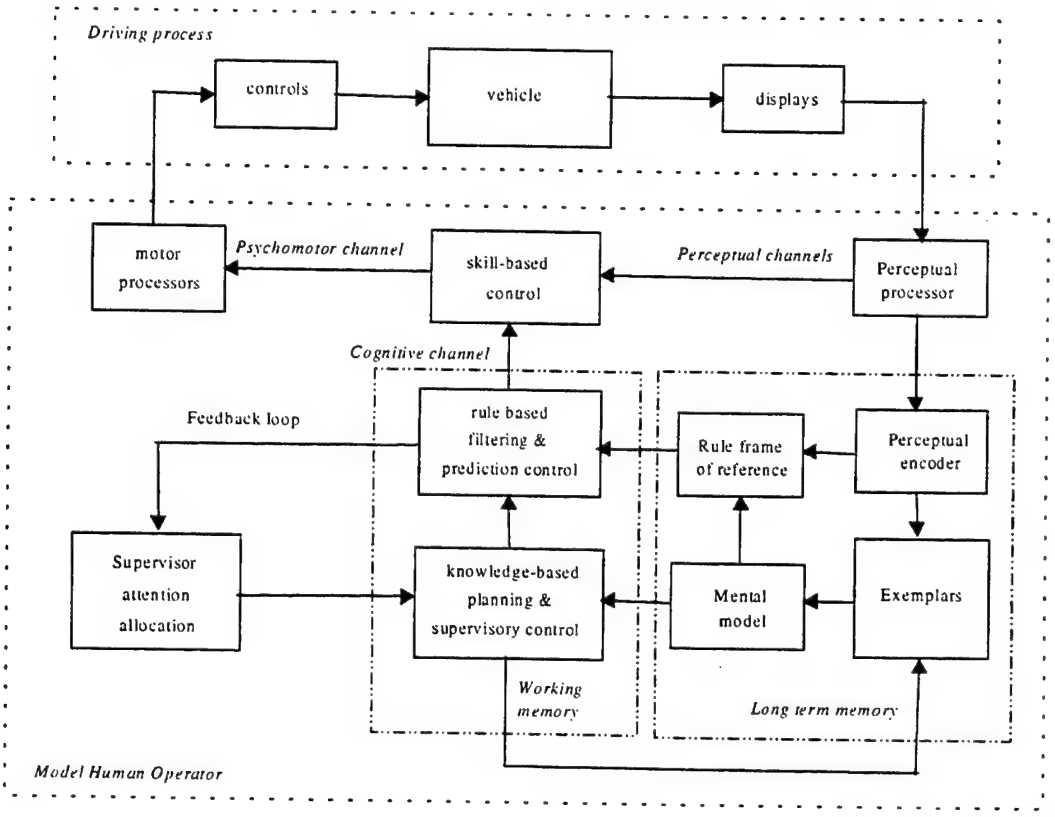

Figure 4. Driver Information Processing Model.

As a controller of the driving process, the human operator is modeled with an automatic inner loop for the skill-based processor and a supervisory outer loop for the cognitive processors. The automatic inner loop "pipelines" the parallel activities of the visual perceptual processor, skill-rule response, and motor processor in a predictive "look-ahead" manner, with a refresh interval on the order of 70 ms. The resulting control activity is a sequence of discrete micro-movements executed in bursts of pre-programmed motor instructions with a band-limited response on the order of 14 Hz. While the inner loop is automatic, the outer loop monitors and evaluates the performance for correction by comparing the perceived feedback from the motor response to that expected from the mental model. In this process, the outer loop functions as a serial loop

of eye movement, perceptual processor, rule-based decision, and motor processor, with a refresh interval on the order of 270 ms. For this reason, the bandwidth of the outer supervisory loop is on the order of 4 Hz.

5.3 Micro-State Activity Model

The model for driving operates in a sequence of micro-state processing stages with information flowing through the perceptual processors, a cognitive processor, and motor processors. Time increment and attention loading are associated with each processing step. Information processing is performed at three levels: skills, rules, and knowledge. In the skill level, the perceptual processor is pipelined directly to the psychomotor response with little cognitive processing. In rule-level reasoning, the perceptual information is encoded into a cognitive frame and processed by rules in working memory for motor response selection and evaluation. Finally, in knowledge-level reasoning, associations are made in long-term memory for mapping processing rules and reference frames into the working memory. Although skill-based processing is a direct mapping of template-matched stimuli to psychomotor responses, rule-based reasoning consists of a set of rules containing conditions for stimuli evaluation and the mapping of these conditions to response selections, along with expected results. We argue that skill- and rule-based reasoning are often applied together, with the rule-based reasoning used to monitor the performance of the skill-based processing. A conflict between the stimuli that is expected to result from a course of action and that is actually occurring, results in the application of knowledge-based reasoning for expansion of the frame of reference and rules domain.

Although skill-based processing is a direct mapping of stimuli to response, rule-based processing is based on the encoding of stimuli into a frame of reference and the processing of the rules in working memory. Similarly, knowledge-based reasoning is based on linking the encoded stimuli to associations in long-term memory through working memory. For these reasons, rule- and knowledge-based reasoning are restricted by the time and capacity limitations of working memory retention and by visual and semantic interference between competing stimuli. Although the reference frame dictates the sensitivity to stimuli, the perceptual processors operate independently, encoding stimuli and generating associations in long-term memory as the stimuli are received. Environmental events with concurrent visual and auditory stimuli are processed in perceptual processors. In pipelined action, the perceptual processors may be processing stimuli just received, while the motor processor is executing a response to the last set, and the cognitive processor may be evaluating the response to the set received before that.

Although we have described the response to external stimuli, internal sources of stimuli compete for attention. For example, a conflict between body movement and the visual scene generates a somatic awareness through an additional perceptual processor. Concurrent with the somatic perception is a head

movement by a driver experienced with the indirect vision system, to counter the sensations through opposing movements of the vestibular system. However, the head movement response is based on the previous visual image, and the residual somatic sensation is evaluated in a following cognitive activity at the rules level. Furthermore, attention is redirected by anxiety from subjective stress (Fatkin & Mullins, 1995) that is related to the "chunking" of features for encoding in working memory. In particular, subjective stress is generated by the number of stimuli features being processed in working memory. In turn, the stress level dictates the chunking level for the features and thus the level of knowledge-based associations. For example, a high stress level from novel stimuli with many features may lead to a gross chunking level that maps to recognition-primed decision type associations commonly used by experienced personnel to address or handle stressful situations (Zsambok & Klein, 1997).

6. Application to the Driving Task

A variation of the information processing model is described for the driving task used in the experimental study. The mental model of the driver and his or her task production rules are described for the rule-based processor of the driving model.

6.1 Task Information Processing

The information processing cues are described for the driving task used in the experiment and related to the functions and tasks.

6.1.1 Task Description

Considering a driving course designated by pairs of markers, the driver navigates the course from the locations of the marker pairs in the scene and by recalling his or her knowledge of the route from a mental map of the course. This is followed by a task-specific rule-based selection of the next marker pair and an approach path to the pair. Finally, the driver executes skill-based driving of the vehicle along the approach path and between the marker pair with speed control based on the velocity flow field of the scene and then repeats the process.

As with any driving task, vehicle control at the skill-based level may be thought of as a two-dimensional tracking task with lateral control to maintain lane position and longitudinal control for speed. Lateral control is a second order tracking task with prediction based on a preview of the course ahead and the heading of the vehicle. Longitudinal control is a first order tracking task with command input given by the internal goal of the driver and by the disposition of the road markers. The tracking display presents three channels of visual command information to be tracked along two axes. Lateral tracking is commanded by the course, while longitudinal tracking is commanded by a

distributed set of input consisting of the flow of motion along the course and the distances to the markers. To drive proficiently, the driver needs to see the course ahead within a primary visual attention lobe of forward vision, which extends from a few meters ahead of the vehicle to a few hundred meters directly in front (Wickens, Gordon, & Liu, 1998).

Although this is a valid description of highway driving, the road course used in this study was a successive sequence of short lane segments gated by the marker pairs. For this reason, navigation of the course employed the cognitively demanding rule- and knowledge-based levels to help the participant find the next set of markers and the following lane segment and to prepare and monitor the skill-based looking and control acting activities used for lane passage.

6.1.2 Display Information Sources

Figure 5 is a sketch of a driving scene showing the different visual display elements that the driver uses in decision making during a trial in our experiment. Since the vehicle-mounted camera array looks down on the roadway, the display shows the markers of the closest pair as farther apart, lower on the display, and larger than those farther away. A perspective of the route is outlined on the display by a succession of marker pairs with the markers of each successive pair appearing closer together, smaller, and higher up in the scene.

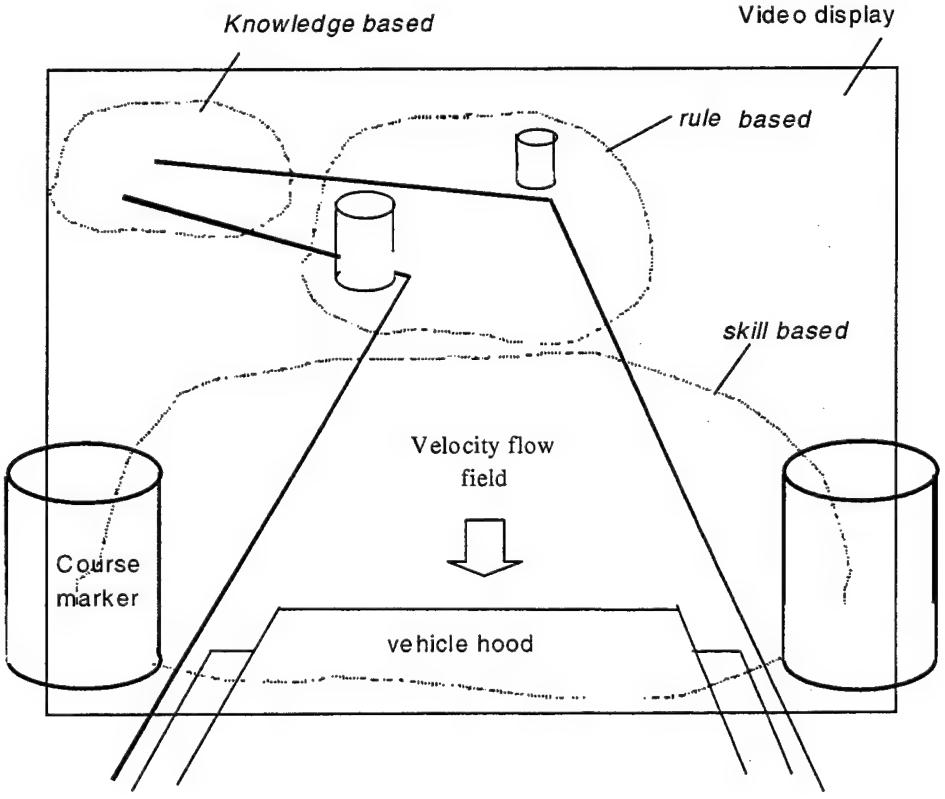

Figure 5. Driving Scene for Experimental Trial.

Superimposed on the scene are encircled elements that correspond to the types of decisions made by the driver. For example, an over-trained, automatic skill-based reasoning acquired from driving one's automobile is used to steer around roadway obstacles as the vehicle approaches them in the vision field. A rule-based, schematic reasoning acquired in training is used to select the next marker pair, the approach path, and speed from the display. The velocity flow field of the display, which shows the movement of the vehicle, originates from this region since it is here that terrain details become large enough to be visible and appear to flow past the vehicle. Finally, a supervisory, knowledge-based reasoning associated with the far scene is used to monitor the rule-based schema and as the course is traveled, restructure it for changing driving conditions.

6.1.3 Allocation of Functions and Tasks

Following this reasoning, Table 1 is a function and task allocation chart proposed for driving the road course. Table 1 allocates the tasks to the resources of the human operator, the operator interface, and the mental model of the process. The chart lists processors for the perceptive, cognitive, and motor activities of the human that are exercised by the performance of tasks. The column of the chart for the operator interface lists the event in the driving scenario that elicits each task, the portion of the scene showing the display cue needed for the subsequent action, the cue feedback from the display, and the response by the driver. Finally, the portion of the mental model that is exercised with the task is listed as situational or task specific. The situational mental model refers to course localization and is based on a mental map of the course. Here, situational awareness is the awareness of the location and orientation of the vehicle on the course and the location of the next marker pair. The task-specific mental model refers to the procedural knowledge used to operate the vehicle between marker pairs. Referring to Table 1, the function of operating the vehicle is separated into three tasks: navigating, approaching, and driving between the marker pair. Following marker passage, the driver navigates by finding the nearest pair on the course from the far scene on the display and his or her mental map of the course and then selects the approach path. He or she then drives the vehicle along the approach path, using the velocity flow field on the front scene to judge speed until he or she nears the marker pair. The driver then steers, using the near scene to align on the pair and accelerates between them to drive through.

6.1.4 Body Movement Behavior

By itself, body movement relative to a visual scene causes the participant to momentarily evaluate his or her mental model of position in the scene. As shown in Figure 6, body movement imposes an additional subtask in the situational awareness domain that is time shared with the procedures of the structured task. In this process, motion sickness forces a monitoring of discomfort awareness as a secondary task competing for attentional resources. In some cases, motion sickness dominates the responses, causing the participant to momentarily discontinue the primary task of driving. While the effect of total severity may be

interpreted as the imposition of an additional monitoring subtask, the corresponding symptoms may have masking effects on the separate attention-processing channels. In this sense, the symptoms of motion sickness are degrading stressors that act as performance-shaping functions for the allocation of attention to the processing channels. For example, the oculomotor symptom may interfere with the visual processing channel, while the disorientation symptom may interfere with the cognitive channel through the impact on situational awareness, and finally, the nausea symptom may appear to be an added attention loading on an activated somato-sensory channel that is otherwise dormant (Ebenholtz, 1992; Kennedy, Fowlkes, & Hettinger, 1989).

Table 1. Allocation of Functions and Tasks

	Human operator						Human operator interface			Mental model	
	Perceptual		Cognition		Motor		Eliciting	Interface	Feed-	Ensuing	Maintenance
Task	visual	skill	rule	memory	ocular	manual	event	display	back	action	task situation
Function: Operating vehicle											
Navigation	x	x	x	x	x		thru marker pair	far scene	nearest marker pair	select approach	x x
Approach control	x	x	x		x	x	path selected	front scene	velocity field	brake/ steer on approach	x
Drive through	x	x	x		x	x	near pair	near scene	align-ment on pair	steer/ accel-erate between pair	x

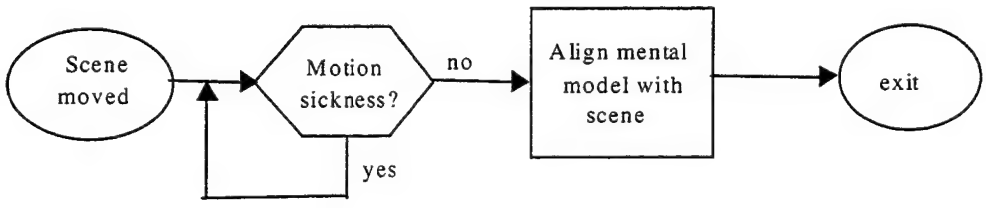

Figure 6. Body Movement Subtask.

6.1.5 Driver's Mental Model

Table 2 lists a mental model for the driving task in terms of goals and actions. In particular, the table lists the goals, operators, methods, and selection (GOMS) rules that could be used in a model of the task (Card, Moran, & Newell, 1983; Kieras, 1988). In this formulation, the human driver has goals that are achieved by specific methods and selection rules. A method is defined as a script sequence of steps that are performed by the perceptual, cognitive, and motor operators. There are usually several methods that need to be performed to accomplish a goal, and selection rules are used to specify the conditions that must be satisfied for a method to be executed (Wickens, Gordon, & Lui, 1998).

For a trained participant, the mental model follows the task analysis. The participant expects to see a sequence of barrel pairs as course markers. Since the participant was driven over the course before the investigation, he or she has knowledge of the course layout in the form of a mental map and does not need to consider route selection. He or she navigates from one pair to the next with a sequence of steering, braking, and accelerating actions to align the vehicle with the next pair before accelerating between them. In this process, the participant sequentially executes a set of selection rules. These rules determine the trial start and end, the course direction, marker pairs, the next marker pair, the approach path, the velocity flow and vehicle speed, the vehicle alignment, and the passage acceleration. A final rule evaluates motion sickness.

Associated with the selection rules are parameters and features used in the decision-making process. Table 3 lists the reference frame held in memory for the parameters and features used with the selection rules of the driving task. The reference values are the values of the features used for the selection criteria. In the driving model architecture of Figure 4, the mental model reference frame is part of working memory with the features' values filled by the perceptual processors as the task is executed. The reference values are established during training. The rule-based processor calls the selection rules according to the task script as each rule is processed in turn. Associated with each selection rule is the set of features and reference values used in processing.

6.1.6 Driving Task Production Rules

The selection rules for the driving task are in the form of conditional production rules that are processed by the rule-based processor. Table 4 lists the production rules for the navigation subtask, the adjust approach subtask, and those for the drive-between-barrels subtask. The production rules are in an "if-then" format where actions are activated (i.e., "fired") when the conditions of the parameters are satisfied. The rules are written with the function calls referring to perceptual and autonomous skill-based processor driven motor activities.

Table 2. GOMS Mental Model of Driving Task

Goal - Transverse course as fast as possible from starting line to finish line by passing between successive pairs of lane markers while committing as few marker strikes as possible.

Operators – On-board manual control of vehicle from visual scene and mental map of road course by using arm and foot movements to operate the steering wheel, accelerator, and brakes.

Method – From the start of the trial to the end, execute a procedure learned in training of first navigating to the next marker pair, adjusting the approach to ensure direct passage, and then passing directly between the markers. The driver navigates by orienting on the course, grouping the barrels into pairs, locating the next marker pair from the visual scene, and then selecting an approach path to the pair that will provide a direct straight through passage. He or she adjusts the approach speed to maintain manual control and then aligns the vehicle with the marker pair. Finally, the driver accelerates between the pair while maintaining control. However, the occurrence of motion sickness forces an evaluation of further participation.

Selection rules - The rules used by the driver in executing the method:

(1) Trial start and end – The trial starts with a verbal command from the experimenter and ends once the last set of barrels is reached.

(2) Course orientation - Direction prompted by driver's mental map of the course and defined on the visual scene by a succession of marker pairs with each pair in the succession smaller and higher on the scene.

(3) Marker pair - Two markers that are most similar in size, about the same level in the display scene, and closest together.

(4) Next marker pair – The pair of markers on course along direction of travel that are closest to vehicle. Since the course is viewed looking downward from an elevated height, the markers of the next pair will appear largest, lowest on the scene, and separated farthest apart.

(5) Approach path - The path of travel that leads the vehicle to a position ending at the next pair that is "head-on" and midway between the two markers. Since the marker pairs are normal to the course, the desired path is estimated from the locations in the visual scene of the next set of markers.

(6) Approach speed - The maximum speed of travel that allows the driver to maintain control during passage over the selected path. The driver locates the velocity flow of the markers and terrain texture in the scene and uses the flow as a measure of the vehicle speed and adjusts the speed to the level learned in training that is appropriate for the vision system.

(7) Vehicle alignment - The location and angular orientation of the vehicle relative to the marker pair; the driver wants the vehicle at the path end point to be midway and aligned normal to the markers for a direct passage without fishtailing or sideward motion.

(8) Passage acceleration - The maximum acceleration in passage between the marker pair that allows the driver to repeat the procedure for the next marker pair by providing sufficient time for task setup before execution.

(9) Motion sickness – If sickness is incapacitating, stop the trial.

Table 3. Mental Model Frame of Reference

Parameter	Features	Reference Values
Course position	mental map location	MAP_LOC
	orientation	MAP_ORIENT
Marker	type	BARREL
	attributes	size, shape, color
Marker pair	differences in sizes	DELTA_SIZE
	levels	DELTA_LEVEL
	spacing	DELTA_SPACING
Next pair	relative size	LARGEST_PAIR
	level	LOWEST_PAIR
	spacing	WIDEST_PAIR
Approach path	curvature	MAX_CURVATURE
	end point	MIDWAY
	end alignment	NORMAL
Scene_blob	position	location, level
	attributes	size, shape, color
Velocity flow field	displacement of terrain texture	TERRAIN_FLOW
	training velocity field	TEMPLATE
Vehicle location	relative to next marker pair	VEHICLE_LOCATION
Vehicle orientation	relative to next marker pair	VEHICLE_ORIENT
Vehicle speed	flow field speed	VEHICLE_SPEED
Task status	idle	IDLE
	determine path	DET
	navigation	NAV
	passage	PASS
Eye field	vision zones on scene	FAR_FIELD
		FRONT_FIELD
		NEAR_FIELD
Glimpse times	present, delayed	NOW, PRIOR
Controller status	accelerator	ACC
	brake	BRAKE
	steering wheel	STEER
Control evaluation	threshold	CONTROL_THRESHOLD
Body awareness	motion sickness	NONE
		SICK
		INCAPACITATED
Run start	verbal command	"Start run"
Run end	finish line	LAST_MARKER_PAIR

Table 4. Production Rules for Driving Course Task

(1). "Map to course" subtask:

IF

// locate barrel markers
// .... expected barrel location?
scene_blob[FAR_FIELD].location ==
recall (marker[BARREL].locations[MAP_LOC, MAP_ORIENT]) *AND*
// .... expected barrel attributes?
scene_blob[FAR_FIELD].attributes ==
recall (marker[BARREL].attributes)

THEN

validate_marker;

IF

// validate paired markers:
// .... nearly same size in scene?
absolute(marker[LHS].size - marker[RHS].size) < DELTA_SIZE *AND*
// .... nearly same level in scene?
absolute(marker[LHS].level - marker[RHS].level) < DELTA_LEVEL *AND*
// .... nearly closest in scene?
absolute(marker[LHS].location - marker[RHS].location) < DELTA_SPACING

THEN

validate_marker_pair;

IF

// confirm next marker pair on route in scene:
// ... largest pair in scene?
pair_size [marker_pair] == LARGEST_PAIR *AND*
// ....lowest level in scene?
pair_level[marker_pair] == LOWEST_PAIR *AND*
// ...greatest separation in scene?
pair_spacing[marker_pair] == WIDEST_PAIR

THEN

assign_next_pair;

ELSE

Reset_search(FAR_FIELD);

(2). "Confirm path" subtask:

IF

// confirm best choice of path locus:
// .. path curvature drivable?
approach_path.curvature [next_pair] <= MAX_CURVATURE *AND*
// .. path ends midway between pair markers?
approach_path.end_postion [next_pair] == MIDWAY *AND*
// .. path ends normal to marker pair?
approach_path.end_alignment [next_pair] == NORMAL

THEN

validate_path_locus;

Table 4 (continued)

```
ELSE
      reset_compute_path_locus;
```

(3). "Monitor approach" subtask:

```
IF
// Isolate velocity field:
// ..... retained attributes of shape, size, color?
     scene_blob[FRONT_FIELD].attributes[NOW] ==
     scene_blob[FRONT_FIELD].attributes[PRIOR]  AND
// ..... moving back?
     absolute (
     scene_blob[FRONT_FIELD].position[NOW]  -
     scene_blob[FRONT_FIELD].position[PRIOR] ) > TERRAIN_FLOW
THEN
     set_velocity_field( match_scene_blobs[FRONT_FIELD] );
IF
// Evaluate approach and adjust manually control:
     absolute (set_velocity_field[NOW] – recall_velocity_field[TEMPLATE] ) >
           CONTROL_THRESHOLD
THEN
     reset_motor_control_for_path(velocity_field);
```

(4). "Monitor passage" subtask.

```
IF
// evaluate alignment of vehicle:
// .... location relative to next pair
     vehicle.location    == next_pair[NEAR_FIELD].location[MIDWAY]   AND
// .... orientation relative to next pair
     vehicle.orientation == next_pair[NEAR_FIELD].orientation[NORMAL]
THEN
     reset_motor_control_for_passage(velocity_field);
ELSE
     reset_motor_control_for_path(velocity_field);
```

(5). "Monitor internal state" subtask.

```
IF
//evaluate somatic state for motion sickness
motion_sickness == INCAPACITATED
THEN
STOP:
ELSE
Continue;
```

7. Mental Workload Measures

The workload measures are reviewed and discussed. The relationship among the measures is analyzed and the dependency of the perceived workload on the other mental workload measures is determined.

7.1 Workload Measures

The mental workload measures used in this study are the product of the previously mentioned field experiment (Smyth, Gombash, & Burcham, 2001), during which subjective evaluations were collected as completed questionnaires from the participants at the end of each driving trial run.

7.1.1 Mental Workload Questionnaires

The questionnaires applied in the field experiment are as follows.

NASA-TLX - The National Aeronautics and Space Administration (NASA)-Task Loading Index (TLX) workload questionnaire (Hart & Staveland, 1988) is used for rating the perceived workload in terms of task demand and interaction. The NASA-TLX is a multidimensional rating procedure for the subjective assessment of workload. The developers of the questionnaire have defined workload as a hypothetical construct that represents the cost incurred by the human operator to achieve a specific performance level. The construct is composed of behavioral, performance, physiological, and subjective components, which result from the interaction between a specific individual and the demands imposed by a particular task. The questionnaire consists of six 9-point (0 to 9) bipolar scales for rating the mental, physical, and temporal demands of the task and the effort, performance, and frustration of the participant (Charleton, 1996).

Allocation of task attention - The questionnaire is used for rating the allocation of attention to the visual, auditory, cognitive, and motor processing channels of the human operator according to loading factors (McCracken & Aldrich, 1984). These loading factors are used in task analysis workload (TAWL) simulations (Allender, Salvi, & Promisel, 1998). The questionnaire consists of a set of four 7-point (0 to 7) bipolar scales for rating the attention loading on each channel, with verbal anchors for corresponding activities overlaid on the scales.

SART - The Situation Awareness Rating Technique (SART) questionnaire is used for rating the situational awareness (Taylor, 1988, 1989; Taylor & Selcon, 1994). The SART questionnaire (Selcon, Taylor & Koritsas, 1991) was designed to measure subjective ratings of non-attentional factors such as domain knowledge or schemata and experience, the cognitive nature of the information received while the task is being performed, and the workload needed to process the information. The questionnaire consists of ten 7-point (1 to 7) bipolar scales for

rating the dimensions of assessment demand, ability, and knowledge. In this study, we refer to situational awareness as the driver's awareness of the location of his experimental vehicle on the driving course during a trial run.

Motion Sickness - The Motion Sickness questionnaire is used for the subjective estimation of motion sickness (Kennedy, Lilienthal, Berbaum, Baltzley, & McCauley, 1989). The questionnaire lists 4-point (0 to 3) bipolar rating scales consisting of verbal descriptors for the 16 symptoms such as general discomfort, eye strain, dizziness, and nausea. Based on data from a factor analysis of simulator sickness experiences, a procedure has been developed (Kennedy, Lane, Lilienthal, Berbaum, & Hettinger, 1992) for reducing the scores to subscales for the symptomatic components of oculomotor stress (eye strain), nausea, and disorientation, and in turn, a measure of total severity.

The Subjective Stress scale - The Stress Scale (Kerle & Bialek, 1958) is used to detect significant affective changes in one's emotional state. The scale is thought to be a measure of the overall "anxiety" or "worry" state attributable to stressful situations. The scale consists of a set of 15 verbal anchors ranked by severity for rating stress that in turn have been mapped to a numerical scale by the developers for data analysis purposes.

7.1.2 Behavioral Interpretation of Measures

The perceived workload is the result of the attention devoted to the separate mental functions needed to drive. These are the needs for allocating attention to the driving task, maintaining situational awareness, monitoring for motion sickness, and the anxiety induced by stress. The perceived workload is the mental workload imposed on the vehicle driver by his or her participation. The workload measure consists of demand and interaction dimensions. Although the demand dimensions separately rate the perceived levels of the perceptual, mental, and physical loading experienced by the driver, the interaction dimensions rate the perceived success of the control applications. In the following, an argument is presented for the measures describing different mental functions that impact perceived workload.

A review of the rating anchors for allocation of task attention suggests that the ratings are limited to the performance of well-defined sequential tasks, such as selecting a radio frequency while flying an aircraft (McCracken & Aldrich, 1984). The task allocations rate the attention that is applied to the human information processors (i.e., channels) to perform the task. These are the vision and auditory perceptual processors, the cognitive processor, and the psychomotor processor. Although the perceptual processors concern association and encoding of stimuli and the psychomotor processor executes the actions, the cognitive processor evaluates and selects actions through working memory. However, the working memory of the cognitive processor can be involved in more engaging tasks, such as a rule-based assessment of the action results and selection of the next course of

action from long-term memory (Warwick, McIlwaine, Hutton, & McDermott, 2001).

The ability to process at this meta-cognitive level depends on the ease with which environmental cues can be assimilated into the mental model of the task (Endsley, 1988). In particular, this ability depends on the ease with which environmental cues can be associated with exemplars in long-term memory, including a course of action and expectancy, the capacity for processing the course of action into task scripts, and the demands by the environment on such processing. The SART questionnaire measures the assimilation ability in terms of demand, capability (i.e., supply), and knowledge dimensions. The demand dimensions describe the perceptual nature of the cues by the number of variables, the complexity of the relations among them, and how quickly the relations are changing. These dimensions determine the perceptual attention needed to track the cues and associate them with the elements of the task mental model. The supply dimensions describe the mental capacity available to process the perceived cues. This capacity is determined by the alertness, the spare mental capacity available, the concentration demanded by the task being performed, and the distribution of attention among competing tasks. The understanding dimensions describe the ease with which cues are assimilated into the mental model as determined by the information associated with the cues and the prior experience. Essentially, an environmental cue that cannot be easily assimilated into the task mental model will force the attention of the cognitive processor to be focused on the cue for further study and evaluation.

Although the SART questionnaire measures the ability to process environmental cues that are external to the task, the motion sickness questionnaire rates the attention to an internal somatic perceptual channel that is induced by the occurrence of motion sickness symptoms. As has been noted, although mild motion sickness results in discomfort, extreme cases can arrest operant behavior, causing the primary task to be momentarily discontinued while full attention is focused on the somatic state. In turn, the subjective stress ratings measure the overall "anxiety" or "worry" state attributable to stressful situations and particularly the stress caused by cognitive loading. Thus, although the motion sickness rating corresponds to the narrowing of task attention capacity caused by the redirection of attention to somatic perception and evaluation, the stress rating is indicative of the cognitive capacity that remains for associating cues in situational awareness.

7.2 Analysis of Mental Workload Measures

We analyze the mental workload measures for significant groupings of the measure dimensions. It is argued that the application of a factorial analysis to the mental workload measures constitute a cognitive loading space, which following rotation, forms a "skills-rules-knowledge" information processing space. The

dependency of the perceived workload dimensions on the SRK components is analyzed and discussed.

7.2.1 Statistical Relationships Among Measures

Table 5 is a correlation matrix for the dimensions of the mental workload measures. The correlation entries are computed with the non-parametric Spearman-rho bivariate statistic by ranks (Dixon & Massey, 1969). This is in place of the parametric Pearson correlation, since a study of the data shows that many of the measures are not in a bivariate normal relationship. Table 5 shows in bold lettering the entries that are significant at the $p < 0.01$ level (two-tailed test). Using this level of probability as a lower boundary, we consider first the interrelations among the dimensions of the measures and in turn, the intra-relations among dimensions between measures.

7.2.1.1 Perceived Workload

All dimensions of perceived workload demand are significantly correlated with each other and with the interaction performance, which is significantly correlated with frustration. While frustration is significantly correlated with mental and temporal demands, effort is not correlated with any of the other workload dimensions. In turn, a comparison between measures shows that the correlation of the workload dimensions to those of the other measures is sparse. However, some workload dimensions are significantly correlated with those of attention loading, situational awareness, the symptoms of motion sickness, and the subjective stress. In particular, the TLX mental demand is significantly correlated with the visual and cognitive channels and the temporal with the visual. Further, all dimensions of workload demand are significantly correlated with those of SART-demand, except for TLX-mental with SART-variability, which is significant at the .05 level. All TLX-demand dimensions are correlated with the SART information quantity, as well as the mental demand with concentration, and the physical with familiarity. While the physical demand is correlated with nausea, the temporal demand is correlated with all symptoms of sickness. The TLX performance is significantly correlated with the visual channel and with SART-complexity and concentration. The frustration is correlated with all SART-demand dimensions, the sickness symptoms, and the subjective stress.

7.2.1.2 Attention Allocations

The visual channel is correlated with all the other channels of attention loading, that is, the cognitive, auditory, and motor channels. However, none of the other channels are correlated with each other. In turn, the visual channel is correlated with SART-complexity and concentration, the cognitive channel with concentration and attention division, and the auditory channel with the information quantity. However, none of the attention loading dimensions are correlated with the motion sickness symptoms or stress.

Table 5. Spearman-rho Correlation Matrix for Mental Workload Measures

		TLX						*Attention loading*				*SART*									*Sickness*			*Stress*
		Demand			*Interaction*			*Channels*				*Demand*			*Supply*				*Understanding*						
		Mental	Physical	Temporal	Effort	Performance	Frustration	Visual	Cognitive	Auditory	Motor	Instability	Variability	Complexity	Arousal	Mental Capacity	Concentration	Attention division	Info Quantity	Info Quality	Familiarity	Nausea	Oculomotor	Disorientation	Subjective stress
TLX	Mental	1.0	**.698**	**.753**	.193	**.938**	**.508**	**.584**	**.488**	.388	.108	**.489**	.430	**.653**	-.005	-.139	**.547**	.229	**.478**	.359	.288	.290	.177	.227	.194
	Physical		1.0	**.783**	.108	**.637**	.340	.391	.400	.369	.064	**.540**	**.584**	**.655**	.112	-.180	.338	.020	**.535**	.401	**.450**	**.561**	.266	.287	.284
	Temporal			1.0	.312	**.734**	**.559**	**.563**	.254	.326	.229	**.638**	**.509**	**.797**	.112	-.288	.348	.041	**.469**	.222	.178	**.633**	**.468**	**.482**	.436
	Effort				1.0	.338	.362	-.031	.072	-.031	.125	.145	.143	.260	-.045	-.140	.210	.237	-.003	-.055	-.073	.248	.169	.120	-.006
	Performance					1.0	**.527**	**.459**	.352	.277	.113	.340	.343	**.554**	.018	-.132	**.573**	.232	.384	.369	.257	.238	.130	.174	.111
	Frustration						1.0	.204	.073	.054	-.089	**.610**	**.664**	**.654**	.112	-.325	.131	-.187	.053	-.172	-.302	**.578**	**.596**	**.576**	**.682**
Attention loading	Visual							1.0	**.555**	**.460**	**.453**	.425	.310	**.532**	.155	.144	**.496**	.293	.308	.275	.225	.206	.149	.158	.248
	Cognitive								1.0	.384	.131	.203	.295	.341	.079	.316	**.658**	**.525**	.435	.427	.370	.061	-.110	-.082	-.069
	Auditory									1.0	.242	.301	.249	.356	.253	.065	.433	.211	**.579**	.350	.364	.017	-.091	-.155	-.019
	Motor										1.0	.074	-.073	.015	-.238	-.270	-.023	.291	-.014	.052	.233	.135	.176	.060	.036
SART	Instability											1.0	**.835**	**.874**	.295	-.338	.058	-.207	.297	-.020	-.002	**.604**	**.545**	**.522**	**.703**
	Variability												1.0	**.785**	.397	-.216	.070	-.253	.194	-.027	-.037	**.563**	.435	.426	**.698**
	Complexity													1.0	.279	-.225	.314	-.128	.403	.115	.086	**.597**	.427	.432	**.593**
	Arousal														1.0	.255	.280	-.415	.378	.304	.128	-.001	-.087	.017	.234
	Mental Capacity															1.0	.348	.264	.030	.157	-.019	**-.440**	**-.585**	**-.490**	-.367
	Concentration																1.0	.362	**.525**	**.661**	**.460**	-.034	-.199	-.158	-.220
	Attention division																	1.0	.022	.077	.100	-.194	-.179	-.234	-.470
	Quantity																		1.0	**.747**	**.653**	.068	-.090	-.062	-.041
	Quality																			1.0	**.819**	-.237	-.337	-.312	-.291
	Familiarity																				1.0	-.072	-.245	-.255	-.344
Sickness	Nausea																					1.0	**.838**	**.839**	**.630**
	Oculomotor																						1.0	**.954**	**.620**
	Disorientation																							1.0	**.640**
Stress	Subjective stress																								1.0

Note: **Bold** entry correlation statistically significant at the 0.01 level (two-tailed test).

7.2.1.3 Situational Awareness

All the SART-demand dimensions are correlated with each other, as are all the SART-understanding dimensions. However, none of the demand dimensions are correlated with any of the supply or understanding dimensions. None of the supply dimensions are correlated with each other; only concentration is correlated with the understanding dimensions. All the SART-demand dimensions are correlated with motion sickness nausea and subjective stress. Instability and mental capacity are correlated with all the sickness symptoms.

7.2.1.4 Motion Sickness

All symptoms are correlated with each other and with subjective stress.

In summary, although some of the dimensions from this study are correlated within a measure and across measures, the correlation is sparse. However, some workload dimensions are correlated among themselves and with the dimensions of attention loading, situational awareness, sickness symptoms, and subjective stress. In turn, the attention loading factors are correlated with a few SART dimensions but not sickness symptoms or stress. Further, some SART dimensions are correlated with themselves, the sickness symptoms, and stress. Finally, although the sickness symptoms are strongly correlated among themselves, the subjective stress is correlated with frustration, SART-demand, and sickness.

7.2.2 Cognitive Component Space

Perceived workload is interpreted as the weighted sum of the attention to (a) the perceptual, cognitive, and psychomotor task-level processors; (b) the perceptual association and cognitive processing of situational cues; (c) induced for monitoring the somatic channel by motion sickness; and (d) anxiety for stress. However, as has been noted before, the task allocation, SART, and motion sickness dimensions are intra-correlated to some degree. For this reason, the derivation of a unique expression for the workload by regression analysis with the stepwise method is difficult because of the collinearity between these measures. One technique commonly used is principal component expansion to reduce the measures to an orthogonal representation of the experimental variance and to perform a regression analysis on the resulting basic set (Neter, Kutner, Nachtsheim & Wasserman, 1996). Figure 7 shows a factorial component loading diagram for the task allocation, SART, and MS measures, along with subjective stress, following reduction to three components with a factor analysis with principal component expansion as the extraction method (68.96% total variance explained), and Varimax rotation with Kaiser normalization (Cooley & Lohnes, 1971). Because of the sparse inter-correlation between dimensions, the separate dimensions were used in the analysis. Table 6 lists the rotated component matrix for the factor analysis.

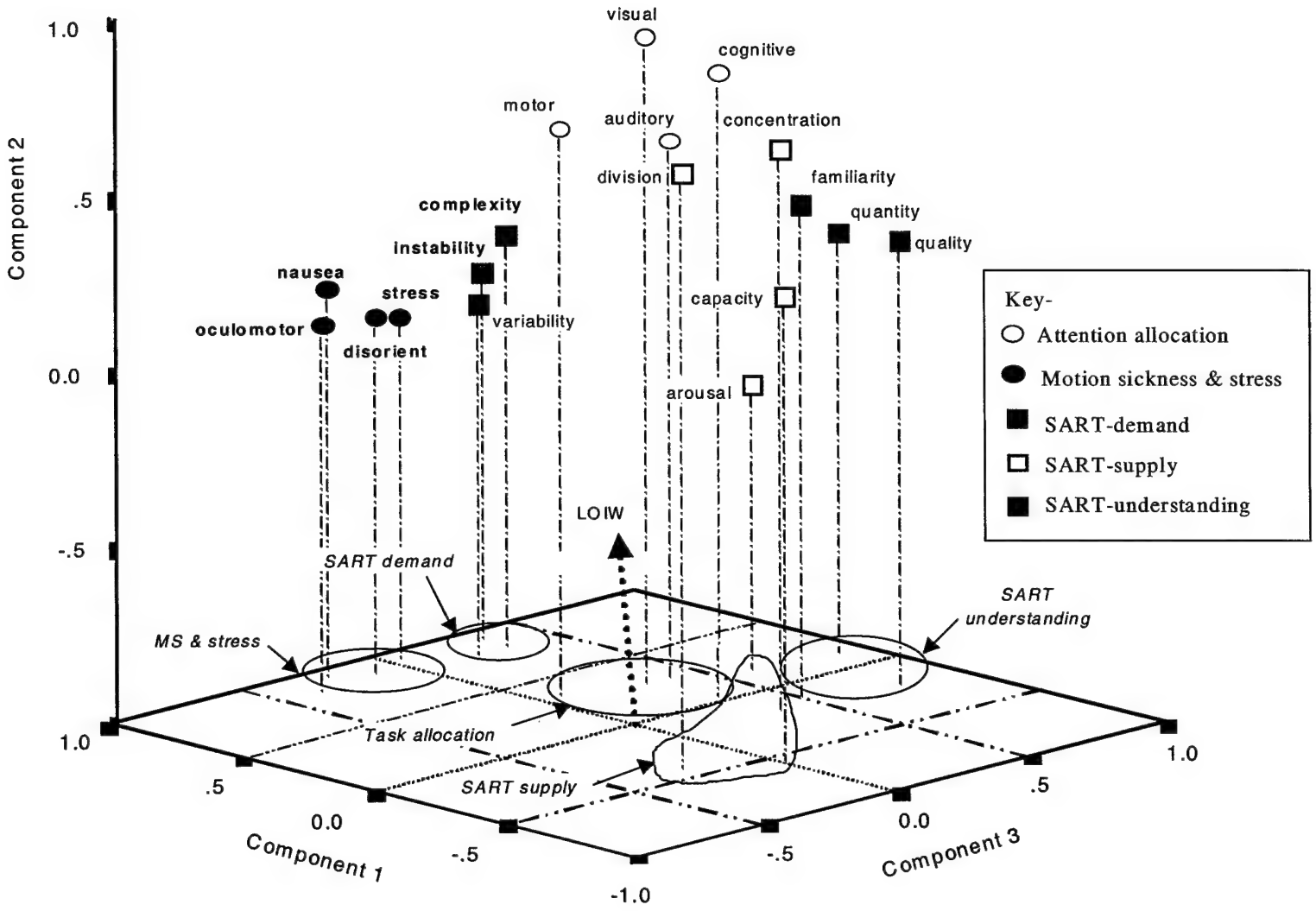

Figure 7. Cognitive Component Space.

Table 6. Factorial Analysis Component Matrix

Measure	Factorial Component First	Second	Third
Task allocation			
Visual	0.132	0.909	0.141
Cognitive	0.030	0.843	0.215
Auditory	0.223	0.577	0.310
Motor	0.185	0.662	-.043
SART			
Demand-			
Instability	0.844	0.164	0.161
Variability	0.804	0.104	0.112
Complexity	0.754	0.327	0.140
Supply-			
Arousal	0.256	-.116	0.606
Capacity	-.646	0.245	-.098
Concentration	-.115	0.632	0.355
Division	-.550	0.615	-.369
Understanding			
Quantity	0.172	0.288	0.789
Quality	-.185	0.222	0.871
Familiarity	-.111	0.005	0.606
Motion sickness			
Nausea	0.905	0.116	-.105
Oculomotor	0.856	0.041	-.124
Disorientation	0.885	0.025	0.101
Subjective stress	0.885	0.048	-.129

7.2.3 SRK Processing Structure

One way of looking at the loading diagram is that it forms a cognitive component space with information processing defined by a cognitive state trajectory. Considering the groupings of the measures, it can be argued that the component axes correspond to levels of cognitive processing. In particular, we argue that the components correspond to the skills, rules, and knowledge levels of reasoning (Rasmussen, 1983, 1986, 1993). In Figure 7, Component 2 corresponds to the skills level, Component 1 to the rules, and Component 3 to knowledge reasoning. This interpretation is based on the following argument.

Notice that the SART-understanding dimensions, which imply knowledge, project to Component 3, with little projection to the other two components. Similarly, the SART-demand components along with the motion sickness symptoms and subjective stress, project to Component 1, with little projection to

the other two components. Here, considering the nature of the dimensions, cognitive demand implies rule-based analysis. Finally, the visual and cognitive attention allocations, which imply task focus, are predominantly aligned with Component 2, while SART demand and motion sickness along with stress, which imply internal focus, have little projection to this component. However, task focus in turn implies skill-based behavior. Further, the SART-supply dimension of arousal that is needed for processing knowledge is aligned with Component 3, while the concentration and division-of-attention dimensions are aligned with Component 2, and capacity with Component 1.

The SRK interpretation is further supported by the fact that the projections of the task attention allocation dimensions are clustered near the intersection of Components 1 and 3, implying that little rule- or knowledge-based reasoning is used in the allocation dimensions. Notice that all SART measures have minimal projection to Component 2, implying little skilled behavior. In turn, Figure 7 shows motion sickness and stress with none of the skills of Component 2, negative knowledge or understanding from Component 3, and a direct rule response for Component 1.

7.2.4 Total Workload

Following the argument just given, the perceived workload is interpreted as a weighted sum of the attention applied to the three levels of reasoning. A correlation of the perceived workload with the factorial components via the non-parametric bivariate Spearman-rho statistic for a two-tailed test shows that the total TLX is significantly correlated with the first ($R^2 = 0.441$, $p = 0.019$, $N = 28$) and second ($R^2 = 0.713$, $p < 0.001$, $N = 28$) components but not the third. Similar correlation values apply to the workload demand and interaction sums. The implication is that the total workload is determined by the attention demanded by the task allocation and the rules processing but not to knowledge processing for this driving task.

Applying curve estimation techniques for relating the workload to the factorial components, the total workload is described by a cubic polynomial with a constant term in the first component and a quadratic polynomial with a constant term in the second but not at all in the third. A linear regression analysis of the total workload as a function of the powers of the first and second factorial components with the entry method (Pedhazur, 1982) is statistically significant (adjusted $R^2 = 0.482$, $p < .001$, $F = 6.033$, $df = 5$, $dfe = 22$); however, none of the coefficients are significant. The entry method produces residuals that are uniformly distributed across component values.

The results of the analysis suggest that perceived workload for this study is a product of skills and rules reasoning but not knowledge-based reasoning. In particular, the total workload index (TTLX) is given by

$$TTLX = -35.933 + 2.924*SKILLS - 3.042E\text{-}02*SKILLS^2 + 3.071E\text{-}02*RULES - 1.723E\text{-}04*RULES^2 + 3.503E\text{-}07*RULES^3, \quad (7)$$

in terms of the first ("RULES") and second ("SKILLS") factorial components, with the coefficients in scientific notation. The factorial components are expressed as a weighted sum of the measures used in the analysis, where the corresponding weights are listed in Table 6. Following Equation (7), the isobars of constant workload form a family of curvilinear lines in the skills-rules plane (defined by Components 1 and 2). These isobars are perpendicular to the locus of increasing workload (LOIW), which for low component values, is practically along the skills axis (Component 2), as shown in Figure 7.

7.2.5 Statistical Values of Components

For modeling workload, the statistical contributions of the factorial components to the workload are of interest. Table 7 lists the averages and standard deviations for the contributions to the total workload from the first two components predicted with Equation (7), as a function of the experimental treatments of direct and indirect vision driving. A study of the statistics for the contribution from the SKILLS component shows that there is no difference by treatments in distributions despite the large difference in number of samples; in particular, the indirect mean is within the 95% confidence interval for the mean of the direct distribution. In contrast, the direct and indirect distributions for the contributions from the RULES component are different; in particular, the mean for one distribution is not bound by the 95% confident interval for the mean of the other. The implication is that the significantly statistical change in workload with treatment is caused by the change in the RULES-component alone. The workloads induced by the SKILLS response are specific to the experimental participant and are cancelled across treatments by the counterbalanced design.

Table 7. Significant Statistics for Total Workload Contributions From the First Two Factorial Components

	Treatment					
	Direct			Indirect		
Component	N	Average	SD	N	Average	SD
SKILLS	6	60.126	8.635	22	64.436	6.393
RULES	6	0.659	0.651	22	2.660	4.287

SD = standard deviation

7.2.5.1 SKILLS Component

A study of Table 6 shows that the major sources of Component 2 are the allocation of task attention and the SART-supply dimensions of concentration

and division. These variables are not significantly different by treatment, and the average values are listed in Table 8 for the task allocations and Table 9 for the SART dimensions. For completion, Table 9 lists the averages for the SART-understanding dimensions that are the major sources of Component 3, as well as those for the remaining supply dimensions and that for the variability dimension a source of Component 1, since none change significantly with treatment. The insignificant changes in these dimensions are the sources of the insignificant changes in the SKILLS-component with treatment.

Table 8. Averages of the Task Attention Allocations

Channel	Loading	Verbal Anchor
Visual	5.372	track, follow, maintain orientation
Auditory	4.812	interpret semantic content of speech
Cognitive	5.453	recall, encode, decode
Psychomotor	5.212	manipulation, discrete adjustment

Table 9. Averages for Statistically Insignificant SART Dimensions

Measures	Average
Demand-	
Variability	4.341
Supply-	
Arousal	4.138
Capacity	4.247
Concentration	5.534
Division	4.772
Understanding	
Quantity	5.694
Quality	5.506
Familiarity	5.231

7.2.5.2 RULES Component

A study of Table 6 shows that the major sources of Component 1 are the SART-demand dimensions of instability and complexity, the motion sickness symptoms, and the subjective stress. Table 10 lists the statistically significant averages for these measures as a function of the experimental treatments. Table 10 shows that the averages for all measures are greater for the indirect viewing treatment. This is the source of the increase in the workload contribution from Component 1 for the indirect vision treatment.

Table 10. Averages for Statistically Significant Measures

Measures	Direct	Indirect
SART		
Demand-		
Instability	3.05	4.30
Complexity	3.60	4.98
Motion sickness		
Nausea	4.77	45.71
Oculomotor	1.90	37.90
Disorientation	1.74	60.32
Subjective stress		
Stress	17.33	29.68

7.2.6 Expected Total Workload

Using Equation (7) for the total perceived workload given previously, we may compute the average expected values from the data for each treatment. Figure 8 is a set of bar column plots of the average predicted total workload as a function of treatment conditions. The figure shows that the average predicted value for the direct viewing treatment is within the 95% confidence interval for the statistically significant average of 24.225 for that treatment. Similarly, the average predicted values for the indirect viewing treatments are within the 95% confidence interval for the statistically significant average of 31.950 for those treatments.

7.2.7 Workload Dimensions

The relations of the perceived workload dimensions to the factorial components are of interest. In this section, we present the results of statistical analyses for the separate dimensions of perceived workload.

7.2.7.1 Mental Demand

A correlation analysis using the non-parametric bivariate Spearman-rho statistic for a two-tailed test shows that the dimension is significantly correlated with the second (R^2 = 0.542, p = 0.003, N = 28) component but not the first or third. Applying curve estimation techniques, the mental demand is described by a cubic polynomial with a constant term in the second component. A linear regression analysis of the dimension as a function of the powers of the second factorial components using the entry method, is statistically significant (adjusted R^2 = 0.427, p = .001, F = 7.701, df = 3, dfe = 24); however, none of the coefficients are significant. The un-standardized coefficients for the analysis are b_0 = -18.170, b_1 = 1.456, b_2 = -2.811E-02, and b_3 = 1.852E-04, where the indices match the

component power. The entry method produces residuals that are uniformly distributed across component values. The results of the analysis suggest that mental demand for this study is a product of skills reasoning but not rule- or knowledge-based reasoning.

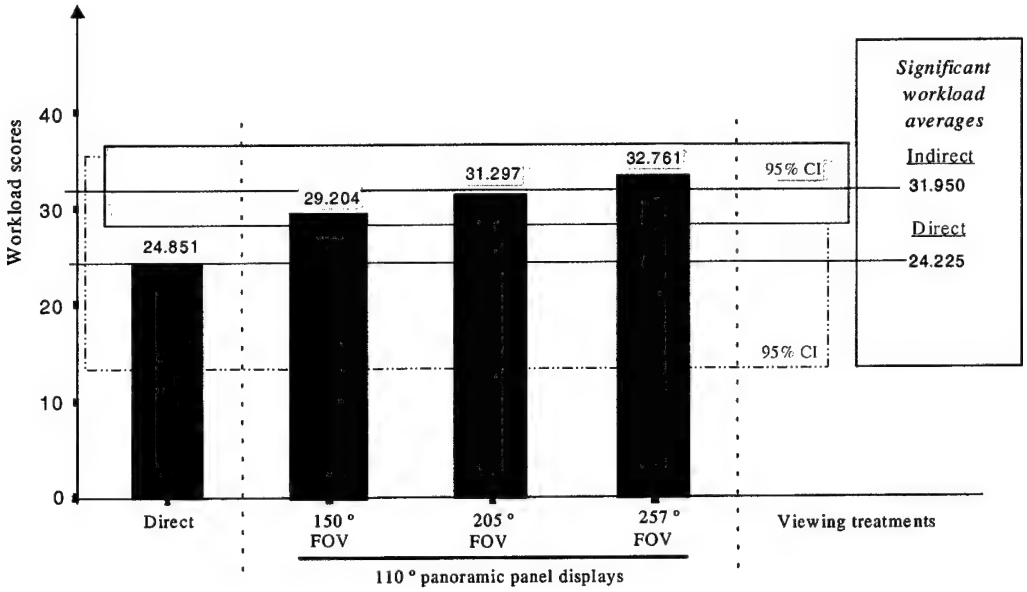

Figure 8. Average Predicted Total Workload for Treatment Conditions.

7.2.7.2 Physical Demand

The dimension is significantly correlated with the second ($R^2 = 0.650$, $p < 0.001$, N = 28) component but not the first or third. The physical demand is described by a cubic polynomial with a constant term in the second component. A linear regression analysis as a function of the powers of the second factorial components is statistically significant (adjusted $R^2 = 0.385$, $p = .002$, F = 6.643, df = 3, dfe = 24); however, none of the coefficients are significant. The un-standardized coefficients for the analysis are b_0 = -7.191, b_1 = 0.560, b_2 = -6.483E-03, and b_3 = 2.226E-05. The results of the analysis suggest that physical demand is a product of skills reasoning but not rule- or knowledge-based reasoning.

7.2.7.3 Temporal Demand

The dimension is significantly correlated with the first ($R^2 = 0.527$, $p = 0.004$, N = 28) and second ($R^2 = 0.774$, $p < 0.001$, N = 28) components but not the third. The dimension is described by a quadratic polynomial with a constant term in the first component and a cubic polynomial with a constant term in the second but not at all in the third. A linear regression analysis is statistically significant (adjusted $R^2 = 0.533$, $p < .001$, F = 7.165, df = 5, dfe = 22); however, none of the coefficients are significant. The un-standardized coefficients for the analysis are b_0 = 7.527, for the constant; b_1 =- 5.828E-03 and b_2 = 4.432E-05, for the first component; and b_1 = 0.844, b_2 = 3.577E-02, and b_3 = 3.980E-04, for the second

component. The entry method produces residuals that are uniformly distributed across component values. The results of the analysis suggest that the temporal demand is a product of skills and rules reasoning but not knowledge-based reasoning.

7.2.7.4 Effort

The dimension is not significantly correlated with any of the factorial components, nor is there any dependency on any power of the components.

7.2.7.5 Performance

The dimension is significantly correlated with the second ($R^2 = 0.441$, $p < 0.019$, $N = 28$) component but not the first or third. The performance is described by a quadratic polynomial with a constant term in the second component. A linear regression analysis as a function of the powers of the second factorial components is statistically significant (adjusted $R^2 = 0.275$, $p = .007$, $F = 6.120$, $df = 2$, $dfe = 25$); however, none of the coefficients are significant. The un-standardized coefficients for the analysis are $b_0 = -4.132$, $b_1 = 0.413$, and $b_2 = -3.682E-03$. The results of the analysis suggest that performance is a product of skills reasoning but not rule- or knowledge-based reasoning.

7.2.7.6 Frustration

The dimension is significantly correlated with the first ($R^2 = 0.708$, $p < 0.001$, $N = 28$), second ($R^2 = 0.562$, $p = 0.002$, $N = 28$), and third ($R^2 = -0.563$, $p = 0.002$, $N = 28$) components. The dimension is described by a cubic polynomial with a constant term in the first component, a quadratic in the second, and a negative linear term in the third. A linear regression analysis is statistically significant (adjusted $R^2 = 0.498$, $p = .002$, $F = 5.468$, $df = 6$, $dfe = 21$); however, none of the coefficients are significant. The un-standardized coefficients for the analysis are $b_0 = 2.494$, for the constant; $b_1 = 1.465E-02$, $b_2 = -9.094E-05$, and $b_3 = 1.373E-07$, for the first component; $b_1 = 7.189E-02$ and $b_2 = 8.896E-06$, for the second component; and $b_1 = -0.144$ for the third component. The entry method produces residuals that are uniformly distributed across component values. The results of the analysis suggest that frustration is a product of skills, rules reasoning, and knowledge-based reasoning.

In summary, the statistical analyses for the separate dimensions of perceived workload as a function of the factorial components interpreted as cognitive levels of reasoning agree with the experimental results reported in the literature (Smyth, Gombash, & Burcham, 2001). This is true except for mental demand which is a function of only the second component and not the first. However, although the mental demand was reported to be significantly different for the experimental treatments, the significance was relatively weak ($p = 0.010$) compared to that for the temporal demand ($p = 0.004$), at least for an analysis of variance (Smyth, Gombash, & Burcham, 2001). Application of the Holm simultaneous testing procedure (Neter, Kutner, Nachtsheim, & Wasserman,

1996) for control of the type I error shows that the separate analyses listed for the total workload and dimensions satisfy a family-wise 0.05 alpha level. The implication is that the separate analyses are statistically significant. This significance does not depend on chance attributable to multiple testing.

7.2.8 Implications for Task Modeling

The results suggest that the perceived workload is a function of what is being interpreted as skill- and rule-based reasoning but not of knowledge-based reasoning. This is reasonable since knowledge of the course and experimental procedure was learned by the participants at the start of the experiment and did not vary with treatments. Furthermore, while the rule-based reasoning is different by treatment, the skill-based reasoning remains statistically consistent. It is interesting that the attention allocation ratings used in this study appear to map to the skills level. However, intense cognitive processing is necessary to support the rules processing and maintain the mental model that is needed for course navigation. One possibility is that rating forms did not include activities as anchors that are pertinent to this level of reasoning. In the next section, we propose a micro-activity model for the skill-, rule-, and knowledge-based reasoning that may be applied to the study performance. The models are used to show that the differences in workload between treatments may be explained by the rule-based reasoning that is needed to monitor the motion sickness during indirect vision driving. Further, the models are used to determine the relations among the ratings for the different measures and particularly the relation of the perceived workload index to the ratings of task allocation of attention.

8. Micro-Activity Time Line Model

In this section of the report, we describe micro-activity time line models for direct and indirect vision driving. In keeping with the literature, human response is assumed to be directed by micro-level activities that occur within cortical based processors, which consist of perceptual processors, a cognitive processor interfacing with memory, and a motor processor (Card, Moran, & Newell, 1983). The processing times are assumed to be on the order of 100 milliseconds (Card, Moran, & Newell, 1983), with a demand loading corresponding to the attention needed to process the information for the task (McCracken & Aldrich, 1984). Furthermore, loading is assumed to be increased by interference that occurs within processors during the performance of concurrent tasks (Little et al., 1993).

Here, skilled reasoning is interpreted as a sequence of over-learned, automatic activities performed in a pipelined manner between connected processors from perceptual to cognitive and then to motor action. In contrast, rule-based reasoning is interpreted as being a cognitive processor activity of an evaluation nature, particularly, of an "if-then" production rule. Finally, knowledge-based

reasoning is interpreted as a cognitive activity involving memory recall and processing. The development of the models is guided by the results of the workload analysis, that is, the skill- and knowledge-based reasoning remains consistent across treatments, while the rule-based reasoning is increased for the indirect vision driving. Further, the activities are restricted to the experimentally derived course times for the treatments. We describe first the model for direct vision driving and then the model for indirect vision.

8.1 Direct Vision Driving

Table 11 is chart of a micro-activity time line for direct vision driving between consecutive sets of course markers. As noted in the activity mode column, the participant, when passing a marker set, first computes the best "satisficing" path (Wickens & Hollands, 2000) to reach the next marker set, then tracks this path, and finally having reached the next set, aligns the vehicle for direct passage and accelerates between the marker pair. The micro-activities performed by the participant during driving are listed in the activity column, and the times when these activities occur are listed in the time column in milliseconds. The time taken to transverse the course segment in the experiment averaged 1.978 seconds (Smyth, Gombash, & Burcham, 2001). The cortical processors involved in these activities are listed in the next set of columns. The time to perform each activity is listed in the interval column, followed by the attention loading and the equivalent verbal anchor. Finally, the workload incurred is listed as the product of attention loading times the processor time interval.

When the participant estimates the path between markers, he is assumed to remember a mental map of the course and to rotate the course section in the cognitive processor for alignment with his or her route of travel. The map recall guides the participant's visual fixation of the next marker set and the redirection of his or her eyes with the motor processor for the fixation of the set beyond those. At this stage, the cognitive load is a result of the need to recall the mental map, encode the map to the scene, and then revise the map by encoding the location. The path to be followed is computed in the cognitive processor following acquisition of the visual locations of the marker sets in the visual perceptual processor.

The participant then drives along the path to the next marker set in a sequence of 100-millisecond pipelined automatic glimpses, path corrections, and control adjustments to stay on course. The marker set is visually fixed by ocular pursuit tracking, which occurs during image acquisition; in contrast, images can only be acquired during a fixation between ocular movements for saccadic vision. The path and control revisions occur concurrently with the visual processing, with the path corrections computed by the cognitive processor via the visual image from the previous glimpse, and the control adjustment by the motor processor from the previous path revision.

Table 11. Micro-activity Time Line for Direct Vision Driving

Mode	Time	Activity	Visual	Cognitive	Motor	Memory	Interval	Loading	Anchor	Workload
Setup path	0	recall map		X		X	70	5.3	decode, recall	0.371
	70	rotate map		X			70	7	estimate	0.49
	140	glimpse	X				100	5	locate	0.5
	240	index eyes			X		100	5.8	discrete adjustment	0.58
	340	glimpse	X				100	5	locate	0.5
	340	index eyes			X		[100]	5.8	discrete adjustment	0.58
	340	compute path		X			70	7	calculation	0.49
track path	410	glimpse	X				100	5.4	track, follow	0.54
	410	index eyes			X		[100]	2.6	continuous adjustment	0.26
	410	estimate path		X			[70]'	7	calculation	0.49
	410	adjust controls			X		[70]"	2.6	continuous adjustment	0.182
repeat 12 times	510	track path								
Finish repeats	1710									17.664
align vehicle	1710	glimpse	X				100	5	align	0.5
	1710	index eyes			X		[100]	5.8	discrete adjustment	0.58
	1710	adjust controls			X		[70]'	5.8	discrete adjustment	0.406
	1810	glimpse	X				100	5	locate	0.5
	1910	confirm		X			70	4.6	evaluation	0.322
Accelerate	1910	adjust controls			X		[70]'	2.2	discrete actuation	0.154
end segment	1980								Total workload = 25.109	

Note: Bracketed times are concurrent.

Once the participant reaches the marker set, he or she continues to visually track the markers and adjust the controls by the motor processor to align the vehicle from the previous image. Then, while confirming alignment by the cognitive processor with the image acquired from a final glimpse, he or she activates the accelerator by the motor processor. Notice that in this model, the confirmation serves as an error check since the action is completed after the motor activates.

The type of reasoning that the activity supports is indicated in the "base" column with the letter "K" for knowledge based, "R" for rule based, and "S" for skill based. Here, we interpret the cognitive action of memory recall and map rotation as being knowledge based reasoning. The path computation and alignment confirmations are conscious processes employing rule-based reasoning. However, the remaining activities are pipelined automatic processes conducted at the skill-based level, which have been established by participants over-training during many years of driving vehicles.

The amount of mental workload incurred in the performance of the activity is indicated in the last column. The workload increment for the processor is the product of the attention loading times the processor interval expressed in seconds. The total workload incurred in driving between consecutive marker pairs is the sum of the workload increments. For direct vision driving, the total workload incurred is 24.563 in units of attention loading times seconds, modeled over a 2.08-second time line.

8.2 Indirect Vision Driving

Table 12 is chart of a micro-activity time line for indirect vision driving between consecutive sets of course markers. The chart has the same format as Table 11, except for the addition of two columns and activities associated with the processing of motion sickness as a second task. Associated with each eye glimpse is the generation of sensory conflict between the visual and sensorimotor activities, which involve the vestibular system through head movements. This sensory conflict is assumed to be perceived by a somatic processor, possibly with associated autonomic responses leading to pallor, drowsiness, salivation, sweating, nausea, and finally, vomiting in the more severe cases of sickness. Concurrent with the somatic perception is a head movement by a driver experienced with the indirect vision system to counter the sensations through opposing movements of the vestibular system. However, the head movement response is based on the previous visual image, and the residual somatic sensation is evaluated in a following cognitive activity at the rules level.

Associated with the performance of concurrent tasks is an increase in attention loading because of interference within and between processors (Little et al., 1993). The increase in loading is expressed as the sum of the separate task loadings times a conflict factor, which is commonly 0.7 for interference within a processor and 0.5 for interference between the visual and cognitive processors

Table 12. Micro-activity Time Line for Indirect Vision Driving

Mode	Time	Participant	Task	Base	Somatic	Visual	Cognitive	Motor	Memory	Interval	Loading	Anchor	Workload
setup path	0	recall map	1	K			X		X	70	5.3	recall	0.371
	70	rotate map	1	K			X			70	7	estimation	0.49
	140	Glimpse	1	R		X				100	5	locate	0.5
	140	Conflict	2	S	X					[100]	4.2	selective orientation	0.42
	140	shift head	2	S				X		[70]'	2.6	continuous adjustment	0.182
	240	Resolve	2	R			X			70	6.8	evaluation	0.476
	310	index eyes	1	R				X		100	5.8	discrete adjustment	0.58
	410	Glimpse	1	R		X				100	5	locate	0.5
	410	index eyes	1	R				X		[100]	5.8	discrete adjustment	0.58
	410	Conflict	2	S	X					[100]	4.2	selective orientation	0.42
	410	shift head	2	S				X		[70]'	2.6	continuous adjustment	0.182
	510	Resolve	2	R			X			70	4.6	evaluation	0.322
	580	compute path	1	R			X			70	7	calculation	0.49
track path	650	Glimpse	1	S		X				100	5.4	track, follow	0.54
	650	index eyes	1	S				X		[100]	2.6	continuous adjustment	0.26
	650	Conflict	2	S	X					[100]	4.2	selective orientation	0.42
	650	shift head	2	S				X		[70]'	2.6	continuous adjustment	0.182
	650	estimate path	1	S			X			[70]'	5.3	recall	0.371
	650	adjust controls	1	S				X		[70]"	4.6	manipulation	0.322
	650	interference	2	R				XX		[70]	5.04	adjustments	0.3528
	750	Resolve	2	R			X			70	4.6	evaluation	0.322
	750	interference	2	R			XX			[70]	6.93		0.4851
	750	interference	2	R		X	X			[70]	5		0.35
repeat 8 times	820	track path											
finish repeat	2180												28.839
align vehicle	2180	Glimpse	1	R		X				100	5	align	0.5
	2180	index eyes	1	R				X		[100]	5.8	discrete adjustment	0.58
	2180	Conflict	2	S	X					[100]	4.2	selective orientation	0.42
	2180	shift head	2	S				X		[70]'	2.6	continuous adjustment	0.182
	2180	adjust controls	1	R				X		[70]'	5.8	discrete adjustment	0.406
	2280	Resolve	2	R			X			70	4.6	evaluation	0.322
	2350	Glimpse	1	R		X				100	5	locate	0.5
	2350	Conflict	2	S	X					[100]	4.2	selective orientation	0.42
	2350	shift head	2	S				X		[70]'	2.6	continuous adjustment	0.182
	2450	Confirm	1	R			X			70	4.6	evaluation	0.322
accelerate	2450	adjust controls	1	R				X		[70]'	2.2	discrete actuation	0.154
	2520	Resolve	2	R			X			70	4.6	evaluation	0.322
end segment	2590											Total workload = 41.900	

Note: bracketed times are concurrent.

(Allender, 1998). Here, we expect interference within the motor processor between control adjustments for driving and head shifting for the motion sickness response through the linkage between the neck and shoulder muscles. Furthermore, we expect interference within the cognitive processor for sickness resolution because of the previous priming for path estimation. Similarly, we expect interference between the visual and cognitive processors during sickness resolution because of previous associations for path estimation.

Notice that the model proposed here for indirect vision driving follows the dictates of the data analysis of workload presented before. Although the knowledge-based activities remain consistent across models, the driving task skill-based activities are changed little, with the path tracking activities taking 13 100-millisecond pipelined sequences for the direct driving and nine such sequences for the indirect vision driving. The increase in driving time for the indirect vision driving is spent in response to motion sickness. However, the addition of the motion sickness response task has greatly increased the rule-based activities. Considering the total workload in driving between consecutive marker pairs as the sum of the workload increments, the total workload incurred for indirect vision driving is 41.333 in units of attention loading times seconds, modeled over a 2.59-second time line as compared to the average experimental time of 2.508 seconds.

8.3 Relation to Mental Workload Measures

From the model structure, we determine the relations of the ratings for the micro-activity time line models to the mental workload measures of allocation of task attention, situational awareness, motion sickness, and subjective stress.

8.3.1 Allocation of Task Attention

As has been mentioned before, the loading ratings reported by the experiment's participants for the measures of the allocation of task attention are statistically independent of the treatments. In the SRK processing structure described previously, the ratings of allocated attention dominate the SKILLS component. In Tables 11 and 12 for the micro-activity models, the skill activities are applied to the track path portion of the time line. In particular, the sequence of a perceptual glimpse and associated visual tracking with path estimation and adjustment of steering controls is interpreted as a skill activity in both models. Essentially, the reported ratings of allocated attention are considered to apply to the driving task, which is the same for both models. The average loading of the model for a channel performing a skilled activity is computed as the total incurred workload divided by the total time needed by the channel to perform the activity. For model verification, this loading may be compared to the rating scores reported for that channel by the participants in the experiment.

Table 13 compares the attention loading of the channels for the model to those reported in the experiment. The table shows that the model-derived loading of

5.400 for the visual channel is close to the average reported value of 5.372 and within the 95% confidence interval for the rating mean (5.804, 4.940). Similarly, the model-derived loading of 5.300 for the cognitive channel is close to the average reported value of 5.453 and within the 95% confidence interval (5.986, 4.920). In addition, the model-derived loading of 5.190 for the psychomotor channel is close to the average reported value of 5.212 and within the 95% confidence interval (5.627, 4.798). The workload for the psychomotor channel is the sum of the skilled activity eye tracking and the control adjustments. The results suggest that the ratings reported for the task-allocated attention agree with those used in the models and that the driving task is consistent across both models.

Table 13. Attention Loading Computations for Skill Channels

Channel	Statistics		Direct Vision Model			Indirect Vision Model		
	Mean	SD	Loading	Time	Workload	Loading	Time	Workload
Visual	5.372	1.197	5.400	1.30	7.020	5.400	0.90	4.860
Cognitive	5.453	1.476	5.300	0.91	4.823	5.300	0.63	3.339
Psychomotor	5.212	1.149	5.190	1.30	6.747	5.190	0.90	4.671

Sample size N = 32 for all statistics.

8.3.2 Situational Awareness

Associated with the immediate task are cue sets, procedures, and expectancies. Skilled tasks have rules associated for assessing the procedure results. Task focus continues at the skilled level as long as the results agree with the expectancies. At the meta-cognition level, cues are naturally noticed and encoded for association in working memory with task employment strategies. These strategies may be reviewed for their effectiveness and a schedule of task implementation formulated. Changes in the cues occur by a conflict between the task results and those expected or by events intruding into the task environment. In addition, the completion of a task generates a rule-based assessment and elicitation of the following task. For example, completion of a course segment by passage between a marker pair elicits the task of calculating the next path as a rule-based activity. In turn, as the next marker pair is approached, a rule-based assessment of the vehicle alignment occurs. Furthermore, motion sickness generates a cognitive need to resolve sensory conflicts that remain after countering head movements. The conflict is resolved by a rule-based cognitive activity that evaluates the course of action.

Although the task allocation describes the task focus at the skill level, the SART ratings measure the awareness to changes in the task environment and the assessment by rules of the strategies for handling these changes. In the SART questionnaire, situational awareness is determined by the demands placed on the

attentional resources by the cues, the capabilities of the resources to process the cues, and the understanding or ease of association with the knowledge base. In our model, these resources are the perceptual processors for encoding the cues, the cognitive processor for association of the encoded cues in working memory, and the rule-based reference frame in long-term memory. In SART, the demands are rated by the cue stimulus properties impacting encoding for associations such as the number of cue variables, the rate of instability or change in the intensities, and the complexity of the relationship among the variables. The demand is higher for a cue with more stimulus variables, faster changes, and complex relationships, since perceptual encoding is more difficult. In SART, the capabilities of the processors are rated by the alertness (i.e., arousal of the senses), the available mental capacity, the ability to concentrate, and the possible spread in focus. In turn, the understanding of the encoded cues is rated by the encoding quality, the encoding quantity, and the familiarity of situation, that is, the value of the knowledge received and understood, amount of knowledge received, and the prior experience.

Here, the objective of this study is to compare the ratings of the SART dimensions to those estimated from the micro-activity models, as determined from the loading of the model processors during rule-based activity. While the SART demand is expressed in cue properties, the micro-activity models presented do not support the resolution of the cue properties for analysis. However, the demand sum may be determined by the loading on the perceptual and cognitive processors of the model during rule-based encoding. In addition, the loading on the motor processor is included because of the effect on result assessment. In contrast, the micro-activity models presented do not support the analysis of the SART dimensions of attention resource capacity (i.e., supply) and the understanding of the situation. These dimensions depend on properties not included in the model. In particular, the cognitive properties, such as the state of alertness, the full cognitive capacity, the concentration and spread of attention focus, are not parameters in these models. Also, the mental model determining understanding is not part of the model. For these reasons, only the SART demand sum is compared.

Referring to Table 11, the sum of the workload incurred for the rule- and knowledge-based processor activity of the direct vision model is 5.973, which equates to an average loading of 7.657 over the 0.78 second. Similarly, referring to Table 12, the workload incurred for the processor activity of the indirect vision model for the driving task and motion sickness is 17.829, which equates to an average loading of 10.550 over the 1.69 seconds. For comparison to the situational awareness ratings, the loading values need to be adjusted for the difference in the rating schemes. Although the task-allocated attention is rated on a 0-to-7 scale (with verbal anchors), the SART dimensions are rated on a 1-to-7 scale. Considering that the SART-demand is the sum of three dimensions, and the direct vision model rule-based workload is summed over three processors, the scaling relation between the two rating schemes is $y = 0.857*x + 3$, assuming a

linear relationship between the equivalent SART-demand (y) and the model loading (x).

With the scaling relation, the equivalent SART-demand for the direct vision model is 9.562; this value is within the 95% confidence interval (14.271, 6.854) for the average demand sum of 10.562 reported by the participants for direct vision driving, according to the statistics in Table 14. Here, the ratio of the demand sum to the model demand is 1.10. Similarly, the equivalent SART-demand for the indirect vision model is 12.041, which is within the 95% confidence interval (15.576, 11.949) for the average demand sum of 13.762 reported by the participants. The ratio of the demand sum to the model demand is 1.14. These results suggest that the SART demand sum is measured by the equivalent demand for the model loading.

Table 14. Comparison of Situational Awareness Demand Sums

	SART Demand Statistics			Model				
Driving Mode	N	Sum Mean	SD	Workload	Time (s)	Loading	Demand	Ratio
Direct Vision	8	10.562	4.435	5.973	0.78	7.657	9.562	1.10
Indirect Vision	24	13.762	4.293	17.829	1.69	10.550	12.041	1.14

8.3.3 Motion Sickness

Motion sickness is interpreted as being caused by the sensory conflicts in the somatic perceptual processor and the associated cognitive assessment. An experienced driver is assumed to naturally move his or her head in such a way as to induce movement of the vestibular system to counter conflicts with the visual scene. However, since the activity is pipelined, the motor activity is in response to a previous visual image instead of the most recent. The result is a skill-based sequence of somatic perception followed by a countering head shift that is generated with each visual glimpse. The conflict remaining is resolved by a rule-based cognitive activity. Since our model does not have the resolution to differentiate between symptom sources, we compare the model to the total severity of motion sickness. Furthermore, since the motion sickness reported was slight for direct vision driving, the symptoms are ignored in the time line of Table 11. Considering the somatic perception, the associated head movement, and the resulting cognitive assessment in Table 12 for the indirect vision model, the total severity loading is 10.342, since the incurred workload is 22.857 over the model time of 2.21 seconds. For comparison to the motion sickness ratings, the loading values need to be adjusted for the difference in the rating schemes. Although the task-allocated attention is rated on a 0-to-7 scale, each of the motion sickness dimensions is rated on a 0-to-3 scale. Although the direct vision model rule-based workload is summed over the three processors for a 0-to-21

scale, the total severity is a weighted sum of the 16 motion sickness dimensions resulting in a 0-to-120.54 scale (Kennedy, Lane, Lilienthal, Berbaum, & Hettinger, 1992). However, the severity distribution for indirect vision is heavily skewed toward lower values (skewness = 1.709, N = 24, standard error = 0.472), and weighting the scale by the ratio of the median (13.980) to the mean (25.998) results in a 0-to-64.82 scale. The scaling relation between the two rating schemes is y = 3.087*x, assuming a linear relationship between the equivalent total severity (y) and the model loading (x). With this relation, the equivalent total severity for the indirect vision model is 31.922, a value within the 95% confidence interval (38.593, 13.403) for the average total severity of 25.998 (N=24, standard deviation = 29.822) reported by the participants.

8.3.4 Stress

Stress is interpreted as being generated by the cognitive load needed to process rules. In the micro-activity time line of Table 11 for direct vision driving, the rule-based reasoning occurs in path computation during the setup path phase and the confirmation during the alignment phase. Considering that the incurred workload is 0.812 over 0.140 second, the model stress loading is 5.80. The average subjective stress reported by the participants for direct vision driving was 12.70, and the ratio of the subjective stress to the model stress loading is 2.189.

In contrast, additional rule-based reasoning occurs in the indirect vision model in resolving the conflict of motion sickness in all phases and the associated cognitive interference during path tracking. This interpretation is supported by the strong correlation of 0.62 between subjective stress and the motion sickness symptoms in Table 5. Considering the micro-activity time line of Table 12, the incurred workload for rules cognitive processing is 12.668 over 1.05 seconds; the model stress loading is 12.065. Since the average subjective stress reported for indirect vision driving was 27.19, the ratio of the subjective stress to the model stress loading is 2.253.

While the rating schemes for the other measures are in fixed bipolar scales, the subjective stress is open ended with no practical limit. For this reason, no relation of the stress rating to the equivalent model loading is derived. However, the ratio of subjective stress to model stress is relatively consistent across the treatments. Assuming that there is no subjective stress when there is no model stress loading (a linear model with zero interceptions), the subjective stress rating scale is about 2.221 that of the model stress loading. In summary, consistent results are produced across driving models by the interpretation of subjective stress as being caused by the cognitive need to process rules.

8.4 Relation to Perceived Workload

We compare the workload incurred for the micro-activity time line models to the perceived workload reported by the experimental participants. We first compare the total perceived workload to the total workload incurred by the micro-activity

model for driving between consecutive marker pairs. We then compare the workload reported for each of the perceived dimensions. Essential to this work is the designation of sources within the model of the workload for the dimensions.

8.4.1 Total Workload

The NASA-TLX of mental workload is interpreted as the perceived task loading over the duration of the task. As described before, the total perceived TLX loading is the sum of the loadings for the measure dimensions. With this interpretation, the workload incurred is the product of the task loading and the course time. Referring to Table 11, the sum of the total workload incurred for the direct vision model is 24.563, which equates to an average loading of 11.809 over the 2.08 seconds. Similarly, referring to Table 12, the total workload incurred for the indirect vision model is 41.333, which equates to an average loading of 15.958 over the 2.59 seconds. For comparison to the total TLX ratings, the loading values need to be adjusted for the difference in the rating schemes. Although the task allocated attention is rated on a 0-to-7 scale, the TLX dimensions are rated on a 0-to-9 scale. Considering that the total TLX is the sum of six dimensions and the model rule-based workload is summed over four processors, the scaling relation between the two rating schemes is $y = 1.928*x$, assuming a linear relationship between the equivalent total TLX-rating (y) and the model loading (x). With the scaling relation, the equivalent total TLX for the direct vision model is 22.768; this value is within the 95% confidence interval (35.271, 13.179) for the average total TLX rating of 24.225 reported by the participants for direct vision driving, according to the statistics in Table 15. Here, the ratio of the total TLX loading to the equivalent model loading is 1.06. Similarly, the equivalent total TLX for the indirect vision model is 30.768, which is within the 95% confidence interval (52.641, 11.259) for the average demand sum of 31.950 reported by the participants. The ratio of the total TLX loading to the model equivalent is 1.04. These results suggest that the total TLX loading is measured by the equivalent model loading. This is interesting since the total loading index is the sum of the demand and interaction dimensions, and only the mental and temporal demands were significantly different statistically by treatment. To remove the baseline effects from the workload computations, we consider the ratio of the differences between the direct and indirect modes for the two approaches; here, a 7.725 difference in the TLX loading and 8.000 difference for the model equivalents result in a 0.97 ratio. That is, the total TLX-loading is measured by the equivalent model loading for the same task.

Table 15. Comparison of TLX Total Workload to Model Total Loading

	TLX Statistics			Model				
Driving Mode	N	Sum Mean	SD	Workload	Time (s)	Loading	Equiv.	Ratio
Direct Vision	8	24.225	13.211	24.563	2.08	11.809	22.768	1.06
Indirect Vision	24	31.950	10.001	41.333	2.59	15.958	30.768	1.04

8.4.2 Workload Dimensions

We consider the relation of the workload dimensions to the micro-activity models. In particular, micro-processor configurations are mapped to the dimensions, and the resulting micro-activity loading values are compared to the rating statistics when possible.

8.4.2.1 Mental Demand

This dimension rates the amount of mental and perceptual activity that is needed to perform the task. We interpret mental demand as the amount of visual perceptual and cognitive activity used at the skill and rule levels to perform the driving task, separate from the somatic response. Referring to Table 11, the sum of the workload incurred for the direct vision model is 14.655, which equates to an average loading of 7.964 over 1.84 seconds. Similarly, referring to Table 12, the workload incurred for the indirect vision model is 11.011, which equates to an average loading of 7.647 over 1.44 seconds. For comparison to the TLX mental demand ratings, the loading values need to be adjusted for the difference in the rating schemes. Although the task-allocated attention is rated on a 0-to-7 scale, the TLX dimensions are rated on a 0-to-9 scale. Considering that the model workload is summed over two processors, the scaling relation between the two rating schemes is $y = 0.6428*x$, assuming a linear relationship between the mental demand rating (y) and the model loading (x). With the scaling relation, the equivalent mental demand is 5.120 for the direct vision model and 4.915 for the indirect vision model. These values are within the 95% confidence interval (6.911, 4.914) for the average mental demand rating of 5.912 reported by the participants (N=32, standard deviation = 2.767).

8.4.2.2 Physical Demand

This dimension rates the amount of physical activity required to perform the task. We interpret physical demand as the amount of skill-based activity used to perform the driving task, separate from the somatic response. Referring to Table 11, the sum of the workload incurred for the direct vision model is 18.589, which equates to an average loading of 14.299 over 1.30 seconds. Similarly, referring to Table 12, the workload incurred for the indirect vision model is 16.612, which equates to an average loading of 18.458 over 0.90 second. Considering that the model workload is summed over three processors, the scaling relation between the two rating schemes is $y = 0.3333*x$, assuming a linear relationship between the physical demand rating (y) and the model loading (x). With the scaling relation, the equivalent mental demand is 4.766 for the direct vision model and 6.153 for the indirect vision. These values are within the 95% confidence interval (6.347, 4.565) for the average physical demand rating of 5.456 reported by the participants (N=32, standard deviation = 2.468).

8.4.2.3 Temporal Demand

This dimension rates the pace at which the task was performed. We interpret temporal demand as the amount of perceptual activity for both the driving task

and the somatic response. Referring to Table 11, the sum of the workload incurred for the direct vision model is 2.000, which equates to an average loading of 5.000 over 0.40 second. Considering that the model workload is summed over two processors, the scaling relation between the two rating schemes is y = 0.6428*x, assuming a linear relationship between the physical demand rating (y) and the model loading (x). With the scaling relation, the equivalent temporal demand is 3.214, which is within the 95% confidence interval (5.107, 1.818) for the average temporal demand rating of 3.462 reported for that treatment (N=8, standard deviation = 1.967). Similarly, referring to Table 12, the workload incurred for the indirect vision model is 15.470, which equates to an average loading of 8.016 over 1.93 seconds. Again, with the scaling relation, the equivalent temporal demand is 5.153, which is within the 95% confidence interval (6.157, 0.451) for the average temporal demand rating of 3.304 reported for that treatment (N=24, standard deviation = 2.019).

Analyses are not made for the TLX interaction dimensions of effort, performance, and frustration, since the micro models do not include appropriate mental modeling as components. The rating of the effort dimension depends on previous experience with the tasks. A participant with more experience requires less effort to perform the same task. The performance dimension rates the participant's perception of his or her success in accomplishing the task goals (as rated by the partiripant). The frustration dimension rates satisfaction with the performance. The evaluation of these dimensions requires inclusion of mental models of experience, goals, and motivation, which are not part of the micro activity models developed here. In the next section, the results of the mental workload analysis are incorporated into a task analysis workload simulation of the driving task. The results are that the task workload is expanded to include additional components of perceived workload in the simulation through the effects of situational awareness, motion sickness, and stress.

9. Task Analysis Workload Simulation

Following the micro-activity models described before, the mental workload is incorporated into a TAWL simulation. In this development, workload is defined as the amount of effort (both physical and psychological) that is expended in response to system demands according to an internal standard of performance (Stein, 1993). Here, driving is a self-paced task and the task load is the speed of travel and the error rate incurred according to the standards established during training. For those participants completing the task, the task load is described in the section about driving speed performance since the field study error rate was effectively constant (Smyth, Gombash, & Burcham, 2001). Mental workload is described in the sections about mental workload measures and micro-activity time line.

9.1 Simulation Modeling Program

The Improved Performance Research Integration Tool (IMPRINT) simulation modeling program (Allender, 1998), which is used to model the workload of the driving task, was developed for ARL by Micro-Analysis & Design, Inc. The program consists of a set of Windows™-based automated aids to assist analysts in conducting human performance analyses. In addition to being useful for estimating crew workload, IMPRINT provides the means for estimating manpower, personnel, and training requirements and constraints for new weapon systems early in the acquisition process.

An essential step in the workload analysis is defining the system mission and the functions and tasks to be performed by the crew in that mission. A hierarchy of task analysis network diagrams is used to depict the functions and the tasks. The network links together the tasks in a sequence of activities with the tasks denoted by the network branches and task completion by the nodes. Depending on the result of a task activity, branching to the next task can occur among tasks connected to the same node. This branching is dictated by a set of branching rules, which may be probabilistic, repeating, or tactical in form. Associated with each task are the specifications for the statistics of the performance time, the accuracy of the result, and the effects on the branching rules. In an advanced version, the task may be subdivided into micro-state activities with associated component times. Also associated with each task are attention loading values for activation of the human visual, auditory, cognitive, and psychomotor information processing channels during task performance and the additional loading attributable to channel conflicts. The attention loading values may be combined into an overall workload measure. Workload management strategies may be designated to handle work overload. The machine displays and controls with which the crew member interfaces are assigned channels as resources that are activated for operations. In turn, the interfaces are assigned to the tasks. Finally, the individual crew members are assigned tasks.

When the simulation model is executed, the tasks are scheduled and performed as specified in the flow diagrams and branching logic. As the tasks are performed, the total instantaneous workload prediction is calculated as the weighted sum of the load on each of the channels at a moment in time as rated with the loading values and a factor that accounts for the amount of conflict between and within resources that are used in parallel. The predicted workload output is a measure of the amount of effort that the tasks, the scenario, and the interfaces are imposing on the simulated operator.

This is, of course, a limited presentation of the full capabilities of the simulation program as it applies to workload for the extremely simplistic task of vehicle driving. This is especially true when compared to the full range of successful application to simulating in-depth operations and maintenance of a wide range of military vehicles and helicopters. However, the construction of a simulation

model allows us to consider perceived workload as an addition to the task workload and particularly, the effects of situational awareness, motion sickness, and stress that result from our field study and consequential analysis.

9.2 Driving Simulation Model

Next, we construct a simulation model for the driving task. We consider the task network diagrams, the resource interface assignments, channel loading values, task activity times, and branching decision rules, and we discuss critical workload.

9.2.1 Task Network Diagrams

Figure 9 is a function-level network flow diagram for the IMPRINT representation of the driving task. The figure shows the trial start, driving the course, and trial end with a probability of an aborted trial because of motion sickness. Figure 10 is a task-level flow diagram for the function of driving the course. The diagram shows the function modeled as an outer loop for navigating between marker pairs, as determined by a branching decision rule, and an inner path for driving the course path between the markers. The rule for the outer loop counts the number of marker pairs that have been passed on the course until the end is reached. The time to traverse the course path is determined from the speed for the vision treatment. In these figures, squares represent higher order functions that are defined by a sequence of tasks that in turn are represented by oval shapes.

In turn, each task in Figure 10 consists of a sequence of subtasks. For the first task in the outer loop (determining the path to drive between marker pairs), the subtasks are mental mapping of the course layout, looking at the far visual field, and selecting the nearest marker pair. These are followed by computing the driving path and looking at the close vision field. Similarly, a subtask flow for the drive function inner loop of driving the computed path consists of the skill-based responses for visually tracking the next marker pair, estimating the path speed, and controlling actions. Finally, a subtask flow for driving between the marker pair consists of a shift to the near vision field and the rule-based responses for aligning the vehicle and accelerator control.

9.2.2 Resource Interface Channels

Table 16 lists the resources and interfaces for the IMPRINT task model. As can be seen from the table, the interfaces of the driver with the vehicle are the visual display and the manual controls. The attentional resources of the driver include the visual, cognitive, and motor channels.

Table 17 shows the relations between the interfaces and resources, that is, which interfaces place demands upon the attentional resources. The table is a simple mapping of the input from the visual display to the visual and cognitive channels and the manual controls as the output of the motor channel.

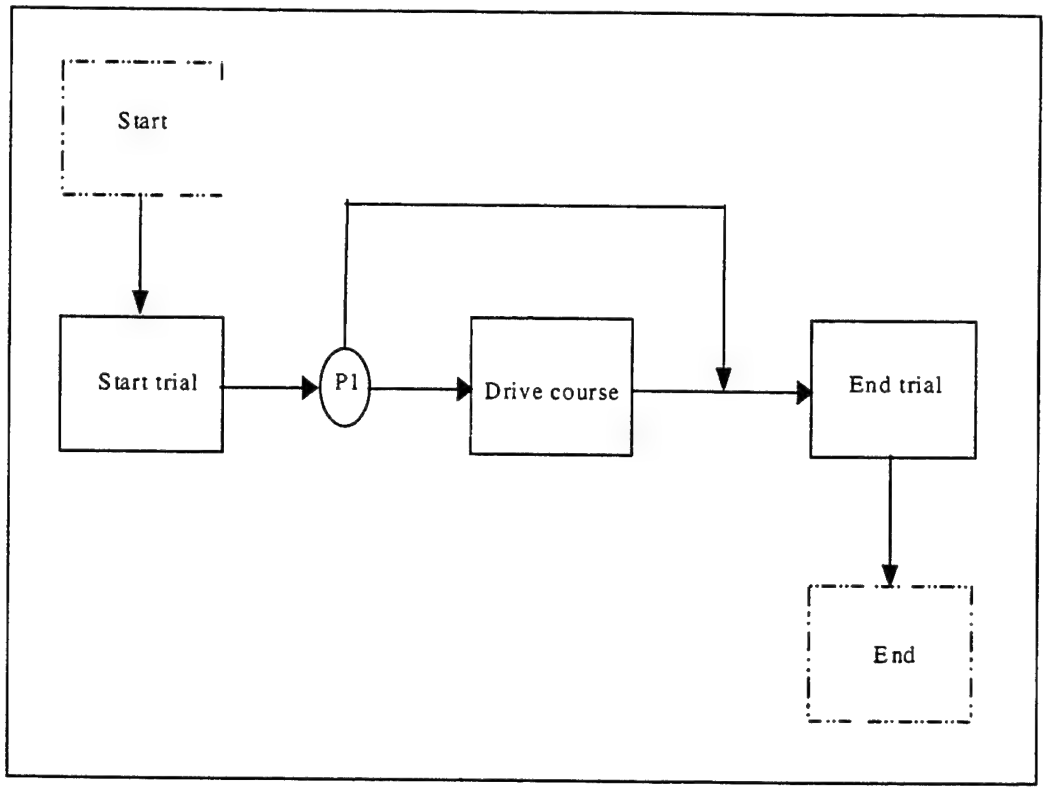

Figure 9. Function-Level Flow Diagram.

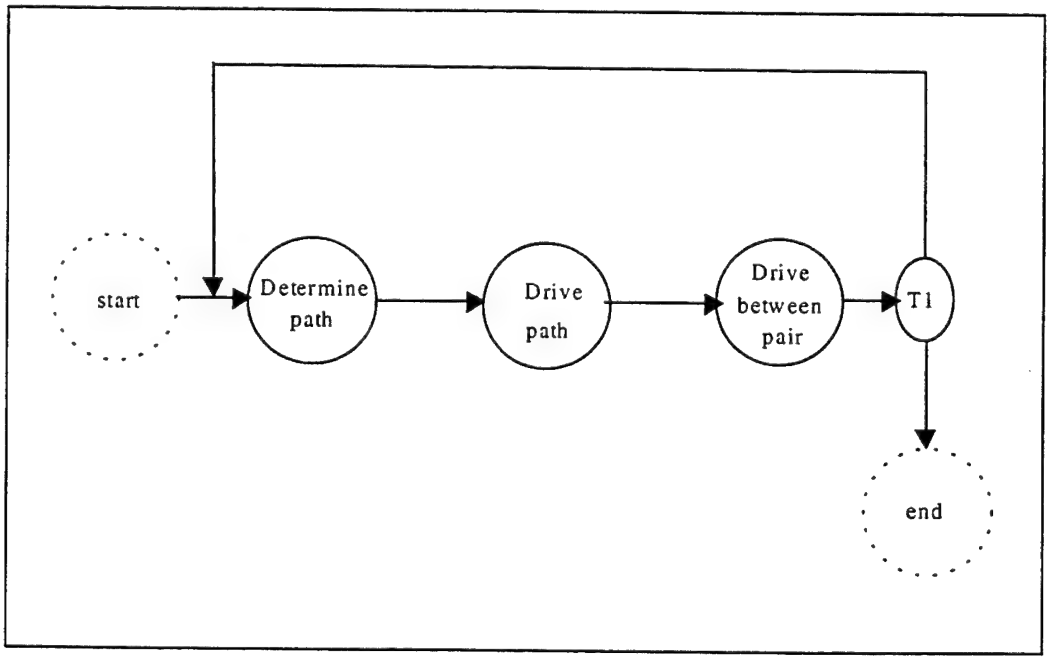

Figure 10. Task-Level Flow Diagram for the Drive Course Function.

Table 16. Workload Attentional Resources and Interface Channels

Resources	Interfaces
Visual	Visual display
Cognitive	Visual display
Motor	Manual controls

Table 17. Relation of Operator Interface Channels to Attentional Resources

Interface	Attention Resources		
	Visual	Cognitive	Motor
Visual display	x	x	
Manual controls			x

9.2.3 Channel Loading Values

Tables 18 and 19 list workload demands placed by the driving tasks upon the resources via the interface channels, for direct vision and indirect vision driving. In the tables, the loading values for the tasks are predicted from the micro-activity models of Tables 11 and 12. In this process, the loading for the task is calculated as the ratio of incurred workload during the task to the time when the loading occurred. In addition to listing the skill-based task allocation and rule-based situational awareness demand for the driving task, the tables list the motion sickness severity and stress. For the driving task, the tables list the loading values on the processors as well as the total loading for the measures. The total perceived work loading is also listed. Further, the experimental values for the measures are listed (in italics), for the course segment over which the tasks occur since they were collected for the trial run and not separately for the tasks. In the micro-modeling section, it was demonstrated that the experimental measures agreed with the loading values derived from appropriate processor configurations for the micro-model time lines following dimension scaling. This is true for all but the subjective stress for which a correction factor was derived since scaling could not be determined. In this manner, the measures are scaled to the 7-point (0 to 7) loading factors scale (McCracken & Aldrich, 1984) used for allocated attention in the IMPRINT simulation modeling.

As computed from Table 11 for the micro-activity model of direct vision driving, Table 18 shows driving rule-based behavior for the first and last tasks and skill-based behavior for the driving path task. The table shows the stress as generated by the loading on the cognitive processor from the situation demand. The skill-

Table 18. Average Attention Loading Values for Direct Vision

Task	Task Allocation				Situation Awareness Demand				Motion	Subject	Total
	Visual	Cognitive	Motor	Total	Visual	Cognitive	Motor	Total	Sickness	Stress	Workload
Determine path	0.0	0.0	0.0	0.0	5.00	6.43	5.80	6.88	0.0	7.00	6.88
Drive path	5.40	5.30	5.19	14.30	0.0	0.0	0.0	0.0	0.0	0.0	14.30
Drive between	0.0	0.0	0.0	0.0	5.00	4.60	6.71	9.12	0.0	4.60	9.12
Course ratings	*5.372*	*5.453*	*5.212*	-	-	-	-	*8.824*	*0.485*	*5.718*	*12.563*

Table 19. Average Attention Loading Values for Indirect Vision

Task	Task Allocation				Situation Awareness Demand				Motion	Subject	Total
	Visual	Cognitive	Motor	Total	Visual	Cognitive	Motor	Total	Sickness	Stress	Workload
Determine path	0.0	0.0	0.0	0.0	5.00	6.14	5.80	6.76	5.89	2.49	8.48
Drive path	5.40	5.30	5.19	14.30	0.0	16.53	0.0	16.53	12.42	16.53	20.84
Drive between	0.0	0.0	0.0	0.0	5.00	4.60	6.71	7.58	10.54	4.60	10.51
Course ratings	*5.372*	*5.453*	*5.212*	-	-	-	-	*12.558*	*10.358*	*12.242*	*16.57*

and rule-based behaviors are de-coupled by task, and the total workload equates to the total allocation loading or the situational demand, depending on the task. Note that in this simulation, the total loading is computed as a weighted sum of the loading values on the processors, in which the weights are the ratio of the duration of the processor activity to the behavior duration for the total loading as determined from the micro-model.

Similarly, as computed from Table 12 for the micro-activity model of indirect vision driving, Table 19 shows rule-based behavior for the first and last tasks and skill- and rule-based behavior for the driving path task. For the latter case, the loading on the situational demand occurs in the cognitive processor and the stress is generated by this loading. Here, the total workload is the accumulation of the task loading, situation demand, and motion sickness.

In each case, the table shows the loading applied to the full task. In concept, the loading specifies the attention demand that is required to perform the mental function during the time that the function is activated as part of the task. As demonstrated in the micro-activity models, a mental function is activated during part of the task and the loading only applies to that period and not to the entire task. However, we may compute the workload incurred as the loading applied over the task duration and summed over tasks; this approach results in workloads that are close in value when one is using the micro-model loading values or values that were experimentally collected. The implication is that we may consider the loading values as applying to the full task duration.

9.2.4 Task Activity Times

Table 20 lists the task activity times for the direct and indirect vision treatments as determined from the micro-activity models of Tables 11 and 12. The total times are the experimentally derived averages for the treatments. These times are used in the simulation.

9.2.5 Branching Decision Rules

Table 21 lists the scenario variables used in the simulation; the status of these variables is used to control the tactical branching logic. Table 22 lists the branching logic for the tactical decision node, T1, of Figure 10. The logic counts the number of marker pairs that have been passed on the course until the course end is reached.

Table 23 lists the logic for the probability node, P1, controlling the task flow between the network functions of Figure 9. The probability is determined by the fact that 2 of the 10 participants in the field experiment chose to discontinue trial runs because of motion sickness. One participant continued the study after a rest, while the other chose to discontinue all further experimental trials because of severe sickness with implications discussed in Section 9.3.

Table 20. Task Activity Times (seconds)

Task	Vision Treatment	
	Direct	Indirect
Determine path	0.51	0.65
Drive path	1.30	1.53
Drive between	0.27	0.41
Total	1.98	2.51

Table 21. Scenario Variables

Variable Name	Type	Role
total_pairs	integer	total number of marker pairs on course
marker_pair	integer	identifier of last marker pair passed

Table 22. Branching Logic for Tactical Decision Node, T1

Purpose: Determine when reached end of driving course.
Method: Count number of marker pairs passed on course.

1. Initialize variables
Function: Start trial
Effect: Beginning

Variable name	value	units
total_pairs	48	integer
marker_pair	0	integer

2. Increment logic:
Function: drive course
Task: drive between pairs
Effect: Ending
Algorithm: marker_pair := marker_pair + 1;

3. Branching logic:
Function: drive course
Task: drive between pairs
Effect: Ending

Following node	logic
Determine Path	marker_pair < total_pairs;
End	marker_pair >= total_pairs;

Table 23. Branching Logic for Probability Node, P1

Purpose: Determine if dropped from course due to motion sickness.

1. Direct viewing

Following node	logic
Drive course	P = 1.0;
End trial	P = 0.0;

2. Indirect viewing

Following node	logic
Drive course	P = 0.8;
End trial	P = 0.2;

9.3 Critical Incident

One question of interest is the critical conditions that if exceeded will cause the driver to abort the trial. Table 24 lists equivalent loading values for the measures reported by the participant who aborted all further trials because of severe motion sickness. This occurred during a driving trial with the near-unity indirect vision system. As can be seen by comparing the table to the statistics in Table 13, although the values for task-allocated attention are slightly higher than the averages, they are outside the 95% confidence ranges for indirect vision, especially those for the visual and motor channels. In contrast, while the situation demand and the perceived total workload are higher, the values are within the corresponding confidence intervals for the rest of the participants. However, the values of motion sickness and subjective stress are about three times greater than the averages for the participants who completed the trials. The motion sickness severity is well outside the corresponding confidence interval, and the stress corresponds to a "frightened" stress state according to the Stress Scale (Kerle & Bialek, 1958). It is interesting to note that although there is an increase in all measures, the increase in task allocations, situation demand, and perceived workload is slight and is within or close to the confidence intervals of the measures for the participants who completed the trials. However, motion sickness and stress increase significantly and as reported, appear to be the source of the aborted trial. The results suggest that the workload has been de-coupled from the motion sickness and stress, and (as reported by the participant) the decision to abort the trial was based on motion sickness alone. Although statistical inferences cannot be made from a single participant, the results suggest a critical limit on the measures for successful task performance. This critical limit may be represented by a hyper-spherical surface in the cognitive component space of Figure 7, the value of which corresponds to an overloaded state, regardless of the source.

Table 24. Critical Attention Loading Values for Aborted Trial Run During Indirect Vision Driving

Task	Resource-Interface Channels: Visual resource display channel	Cognitive resource display channel	Motor resource control channel	Task total	Perceived Components: Situation demand	Motion sickness	stress	Total workload
Course segment	6.902	6.903	6.109	-	14.140	30.732	37.301	17.049

9.4 Simulation Results

Figure 11 shows a representative plot of the predicted mental loading that would be produced by a simulation of the indirect vision driving between sequential marker pairs. The plot shows the loading values from Table 19 for the total task allocation, situation demand, motion sickness severity, stress, and perceived total workload, as a function of the tasks. Superimposed is the critical value of the motion sickness loading from Table 24 that was reported in the previously mentioned motion sickness incident.

9.5 Workload Cost Considerations

Not considered in this study is the effect of long-term demand loading on crew performance. An increase in workload, demand on situational awareness, or the chance of motion sickness may increase the psychological stress on the driver with the indirect vision system. The physiological arousal generated by a high stress level may be detrimental to performance. The immediate effect is to produce a tunneling or narrowing of the perceptual and cognitive attention, with the driver concentrating on the driving task while ignoring the surroundings. There is a tendency toward loss of working memory, with reduced capacity for processing new or complex material and an accompanying focus on well-learned responses and a rapid execution of these responses at the expense of possible errors. The resultant shedding of secondary tasks may not be done in an optimal order for successfully coping with the problem environment. In particular, motion sickness distracts from the task since the discomfort is intrusive and the driver cannot readily concentrate. Although the immediate task performance may be degraded, the long-term effects may be cumulative, resulting in accumulated fatigue over time, which can produce errors and adversely affect performance of subsequent tasks (Wickens, Gordon, & Liu, 1998).

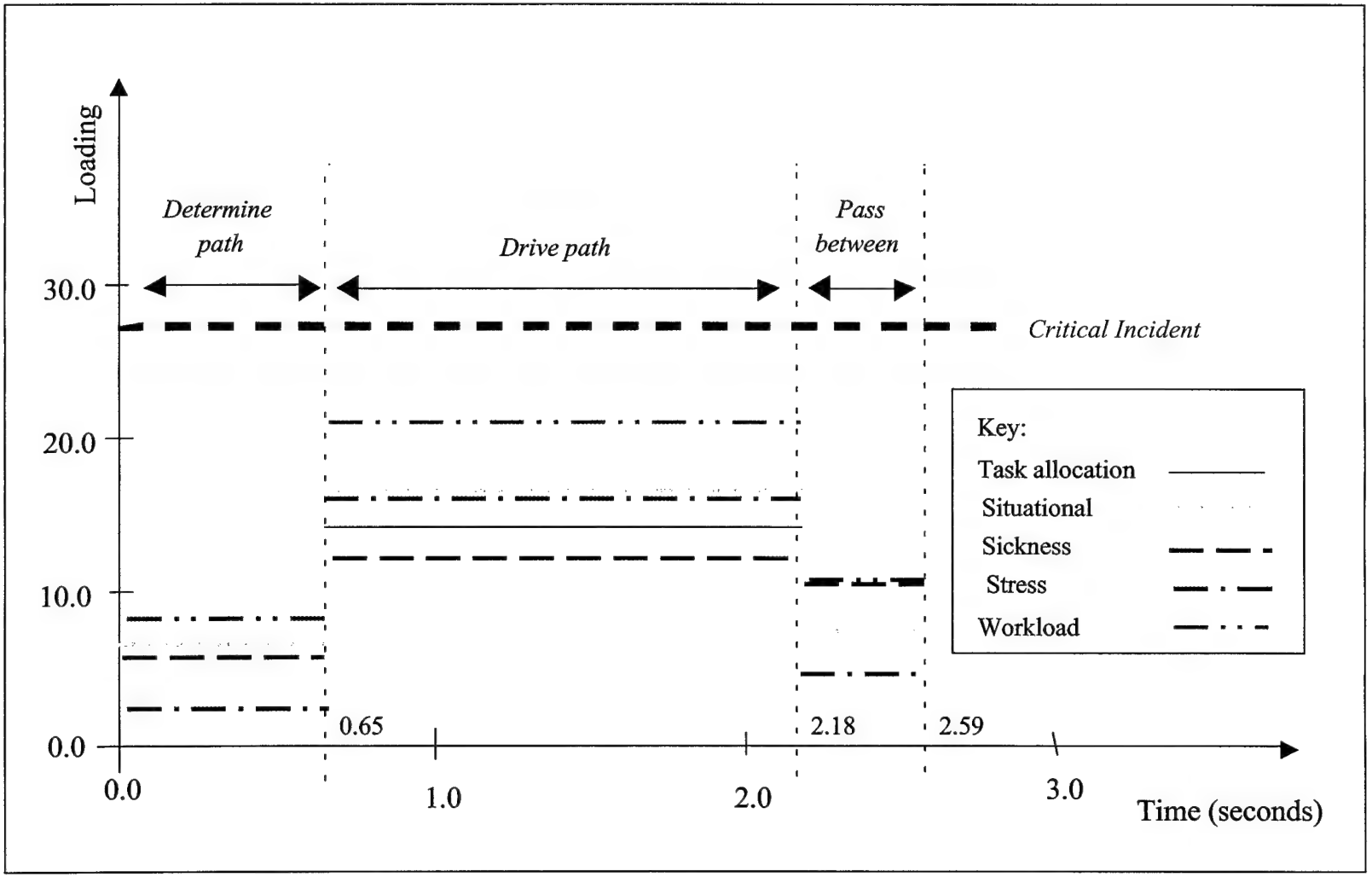

Figure 11. Simulation Output for Indirect Vision Driving Between Sequential Marker Pairs.

10. Conclusions

The perceived workload for indirect vision driving is a function of skill- and rule-based components of reasoning, which is formed from mental workload measures of task attention, situational awareness, motion sickness, and stress, at least for the data collected in our field experiment (Smyth, Gombash, & Burcham, 2001). A factorial analysis of the mental workload measures forms a cognitive component space that corresponds to an SRK model of information processing (Rasmussen, 1983). The measures tend to align with the components, depending on the level of reasoning. For example, the cluster for the task attention loading appears to be associated with a skill-based reasoning that is focused on the driving task without much loading on the rules or knowledge components. In contrast, the motion sickness, stress, and situation demand measures are clustered along the rules component. Finally, the situation understanding measures are clustered along the knowledge component.

The mental workload measures are explained by a micro-state activity model of indirect vision driving that is based on an interpretation of human reasoning as the product of inter-linked perceptual, cognitive, and psychomotor processors (Card, Moran, & Newell, 1983). The model is expanded to include pipelined skilled behavior for driving and body movement to compensate for motion sickness, as well as rule-based behavior for the assessment of situation demand and motion sickness. The development follows a generic information-processing model proposed for driving for which production rules are developed. The results of the cognitive component space analysis are used to further refine the model at the different levels of processing. It is argued that the mental workload measures correspond to different configurations of the model processors activated at the skill- and rule-based level for the tasks of driving and monitoring motion sickness. Of interest is that the loading values generated by the processor configurations significantly agree with the experimental values, following correction for the differences in scaling. Furthermore, significant matching of different configurations of the model processors occurs for the perceived workload and the demand dimensions. The results suggest a common micro-model source for these different facets of human behavior.

The loading values generated by the micro-state model are used in an expanded IMPRINT TAWL simulation modeling program for the inclusion of motion sickness and stress. In this process, the measures are scaled on the 7-point (0 to 7) loading factors scale (McCracken & Aldrich, 1984), used for allocated attention in the program. Note that in this simulation, the definitions of loading, workload, and total loading are tied to the micro-model activity as separate concepts. In particular, total loading is computed as a weighted sum of the loading values on the processors, in which the weights are the ratio of the duration of the processor

activity to the behavior duration for the total loading, as determined from the micro-model. The use of these concepts ensures definite relations between the simulation output and the experimental measures of situational awareness, motion sickness, and stress, as well as perceived workload.

Several issues remain of research interest. Measures from a critical incident involving motion sickness suggest that the perceived workload is uncoupled from the motion sickness during severe conditions and that performance overload can occur for different reasons. This suggests that a critical boundary for overload may be represented by a hyper-spherical surface in the cognitive component space, the value of which corresponds to an overloaded state, regardless of the source.

Another issue is the long-term effect of demand loading on crew performance. An increase in workload, demand on situational awareness, or the chance of motion sickness may increase the psychological stress on the driver with the indirect vision system. While the immediate task performance may be degraded, the long-term effects may be cumulative, resulting in accumulated fatigue over time, which can produce errors and adversely affect performance of subsequent tasks.

Finally, the task load performance and mental workload models derived in this report do not make explicit the higher cognitive processes that are used in driving. A review of the human information processing literature suggests cognitive mechanisms that are needed for a higher level model. The superposition of executive cognitive processes by an expert system consisting of production rules is needed to support the explicit declaration of rule-based reasoning. These higher cognitive processes are used to develop and apply the rule-based schematics that guide and direct the skill-based behavior of driving. An essential element of this supervisory process is the development and maintenance of a mental model of the task and the battlefield situation.

11. Recommendations for Further Research

The author recommends that

- the micro-state model approach developed in this study be used in the analysis of performance and subjective evaluation data collected from experiments. The approach provides insight into the functioning of the human at the information processing level.

- the micro-state model be expanded to include production rules and mental models of the tasks and situation. Further, the model should include training and motivation.

- higher cognitive functions for multiple tasks involving crew interaction and communications and navigation be incorporated. The present study was limited to course driving and did not consider the higher cognitive functions that are required of future combat vehicle operators. The study should include automated adaptive aiding for the performance of multiple tasks in future combat systems.

References

Allender, L.E. (April 1998). *Improved Performance Research Integration Tool (IMPRINT), User's Guide (Version 4.0).* Aberdeen Proving Ground, MD: U.S. Army Research Laboratory.

Allender, L.E., Salvi, L., & Promisel, D. (1998, April). Evaluation of human performance under diverse conditions via modeling technology. In *Improved Performance Research Integration Tool (IMPRINT), User's Guide* (Appendix A). Aberdeen Proving Ground, MD: U.S. Army Research Laboratory.

Baddeley, A.D. (1983). Working memory. In D.E. Broadbent (Ed.), *Functional Aspects of Memory* (pp. 73-86). London: Royal Society.

Baddeley, A.D. (1986). *Working memory.* New York: Oxford University Press.

Baddeley, A.D. (1990). *Human memory: Theory and practice.* Boston: Allyn and Bacon.

Baltzley, D.R., Kennedy, R.S., Berbaum, K.S., Lilienthal, M.G., & Gower, D.W. (1989). The time course of post-flight simulator sickness symptoms. *Aviation, Space, and Environmental Medicine, 60*(11), 1043-1048.

Bekey, G.A., Burnham, G.O., & Seo, J. (1977). Control theoretic models of human drivers in car following. *Human Factors, 19*(4), 399-413.

Brookhuis, K.A., De Vries, G., & DeWaard, D. (1991). The effects of mobile telephoning on driving performance. *Accident Analysis and Prevention, 23*(4), 309-316.

Card, S.K., Moran, T.P., & Newell, A. (1983). *The psychology of human-computer interaction.* Hillsdale, NJ: Lawrence Erlbaum Associates.

Charleton, S.G. (1996). Mental workload test and evaluation. *Handbook of Human Factors Testing and Evaluation,* T.G. O'Brien and S.G. Charlton (Eds.), Mahwah, NJ: Lawrence Erlbaum Associates.

Cooley, W.M., & Lohnes, P.R. (1971). *Multivariate data analysis.* New York: John Wiley & Sons, Inc.

Dixon, W.J., & Massey, F.J. Jr. (1969). *Introduction to statistical analysis.* New York: McGraw-Hill Book Company.

Ebenholtz, S.M. (1992). Motion sickness and oculomotor systems in virtual environments. *Presence, 1*(3), 302-305.

Endsley, M.R. (1988). Design and evaluation for situation awareness enhancement. *Proceedings of the Human Factors Society 32nd Annual Meeting* (pp. 97-101). Santa Monica, CA: Human Factors Society.

Endsley, M.R. (1993a). A survey of situation awareness requirements in air-to-air combat fighters. *The International Journal of Aviation Psychology, 3*(2), 157-168.

Endsley, M.R. (1993b). Situation awareness and workload: Flip sides of the same coin. *Proceedings of the 7th International Symposium on Aviation Psychology,* 906-911. Columbus, OH: Ohio State University.

Endsley, M.R. (1995). Toward a theory of situation awareness in dynamic systems. *Human Factors, 37*(1), 32-64.

Endsley, M.R. (1996). Situation awareness measurements in testing and evaluation. *Handbook of Human Factors Testing and Evaluation,* T.G. O'Brien and S.G. Charlton (Eds.), Mahwah, NJ: Lawrence Erlbaum Associates.

Endsley, M.R. (1997). The role of situation awareness in naturalistic decision making. In C. E. Zsambok and G. Klein (eds.), *Naturalistic decision making* (pp. 269-283). Mahwah, NJ: Lawrence Erlbaum Associates.

Fatkin, L.L., & Mullins, L.L. (1995). Stress, overload and performance: High standards or high stakes. *Proceedings of American Psychological Association-National Institute of Occupational Safety and Health (APA-NIOSH),* February.

Gordon, S.E. (1997). *An information-processing model of naturalistic decision making.* Presentation at Annual Meeting of the Idaho Psychological Association, Sun Valley, Idaho.

Hart, S.G., & Staveland, L. (1988). Development of the NASA Task Load Index (TLX): Results of empirical and theoretical research. In P.A. Hancock and N. Meshkati (Eds.) *Human Mental Workload,* pp. 139-183. Amsterdam: North-Holland.

Hess, R.A., & Modjtahedzadeh, A. (1990). A control theoretic model of driver steering behavior. *IEEE Control Systems Magazine,* August 3 through 8.

Kennedy, R.S., Fowlkes, J.E., & Hettinger, L.J. (4 September 1989). *Review of simulator sickness literature* (TR 89-024, p. 51). Orlando, FL: Naval Training Equipment Center.

Kennedy, R.S., Lane, N.E., Lilienthal, M.G., Berbaum, K.S., & Hettinger, L.J. (1992). Profile analysis of simulator sickness symptoms: Application to virtual environment systems. *Presence, 1*(3), 295-301.

Kennedy, R.S., Lilienthal, M.G., Berbaum, K.S., Baltzley, D.R., & McCauley, M.E. (1989). Simulator sickness in U.S. Navy flight simulators. *Aviation, Space, and Environmental Medicine, 60*, 10-16.

Kerle, R.H., & Bialek, H.M. (1958). *The construction, validation, and application of a subjective stress scale* (Staff Memorandum Fighter IV, Study 23). Presidio of Monterey, CA: U.S. Army Leadership Research Unit.

Kieras, D.E. (1988). Toward a practical GOMS model methodology for user se interface design. In M. Helander (ed.), *Handbook of human-computer interaction* (pp. 135-157). Amsterdam: North-Holland.

Kieras, D.E., Meyer, D.E., Mueller, S., & Seymour, T. (1998). *Insights into working memory from the perspective of the EPIC architecture for modeling skilled perceptual-motor and cognitive human performance* (EPIC Tech. Rep. No. 10, TR-97/ONR-EPIC-10). Ann Arbor, MI: University of Michigan, Electrical Engineering and Computer Science Department.

Klein, G., Orasanu, J., Calderwood, R., & Zsambok, C.E. (eds.) (1993). *Decision making in action: Models and methods.* Norwood, NJ: Ablex.

Little, R., Dahl, S., Plott, B., Wickens, C., Powers, J., Tillman, B., Davilla, D., & Hutchins, C. (1993). *Crew reduction in armored vehicles ergonomic study (CRAVES)* (ARL-CR-80). Aberdeen Proving Ground, MD: U.S. Army Research Laboratory.

McAdams, C.C. (1988). *Development of driver/vehicle steering interaction models for dynamic analysis* (Technical Report 13437, AD-A208244). Ann Arbor, MI: University of Michigan.

McCracken, J.H., & Aldrich, T.B. (1984). *Analysis of selected LHX mission functions: Implications for operator workload and system automation goals* (Technical Note ASI 479-024-84). Fort Rucker, AL: Army Research Institute Aviation Research and Development Activity.

Meyer, D.E., & Kieras, D.E. (1997a). A computational theory of executive cognitive processes and multiple-task performance: Part 1. Basic Mechanisms. *Psychological Review, 104*, 3-65.

Meyer, D.E., & Kieras, D.E. (1997b). A computational theory of executive cognitive processes and multiple-task performance: Part 2. Accounts of Psychological refractory-Period Phenomena. *Psychological Review, 104*, 79-791.

Neter, J., Kutner, M.H., Nachtsheim, C.J., & Wasserman, W. (1996). *Applied linear statistical models*. New York: McGraw-Hill.

Norman, D.A. (1988). *The design of everyday things*. New York: Doubleday.

Pedhazur, E.J. (1982). *Multiple regression in behavior research: Explanation and prediction*. Chicago: Holt, Rinehart, and Winston, Inc.

Rasmussen, J. (1983). Skills, rules, knowledge: Signals, signs, and symbols and other distinctions in human performance models. *IEEE Transactions on Systems, Man, and Cybernetics, 13*(3), 257-267.

Rasmussen, J. (1986). *Information processing and human-machine interaction: An approach to cognitive engineering*. New York: Elsevier.

Rasmussen, J. (1993). Deciding and doing: Decision making in natural contexts. In G. Klein, J. Orasanu, R. Calderwood, and C.E. Zsambok (eds.), *Decision making in action: Models and methods* (pp. 158-171). Norwood, NJ: Ablex.

Sanders, M.S., & McCormich, E.J. (1993). *Human factors in engineering and design*. New York: McGraw-Hill, Inc.

Sanderson, P.M. (1991). Towards the model human scheduler. *Human Factors in Manufacturing, 1*(3), 195-220.

Selcon, S.J., Taylor, R.M., and Koritsas, E. (1991). Workload or situational awareness?: TLX vs. SART for Aerospace systems design evaluation. *Proceedings of the Human Factors Society*, 35th Annual Meeting, 62-66.

Shallice, T., Burgess, P., Schon, F., & Baxter, D. (1989). The origins of utilization behavior. *Brain, 112*, 1587-1598.

Shepherd, R.N. (1978). The mental image. *American Psychologist, 33*, 125-137.

Sheridan, T.B. (1992). *Telerobotics, automation, and human supervisory control.* Cambridge, MA: The MIT Press.

Simon, H.A. (1957). *Models of man.* New York: Wiley.

Simon, H.A. (1987). Decision making and problem solving. *Interfaces, 17,* 11-31.

Smiley, A., Reid, L., & Fraser, M. (1980). Changes in driver steering control with learning. *Human Factors,* 22(4), 401-415.

Smyth, C.C., and Whitaker, R.G. (1998). Indirect vision driving study. *Proceedings of the 21st Army Science Conference,* 15-17 June, 497-502.

Smyth, C.C., Gombash, J., & Burcham, P.M. (2001). *Indirect vision driving with fixed flat-panel displays for unity, wide and extended fields of camera view* (ARL TR-2511). Aberdeen Proving Ground, MD: U.S. Army Research Laboratory.

Stein, E.S. (1993). Human operator workload. In M.W. Smolensky & E.S. Stein (Eds.), *Human Factors in Air Traffic Control* (p. 157). New York: Academic Press.

Taylor, R.M. (December 1988). Trust and awareness in human electronic crew teamwork. In T.J. Emerson, M. Reinecke, J.M. Reising, and R.M. Taylor (Eds.) The human–electronic crew: Can they work together? *Proceedings of a joint GAF/USAF/RAF workshop, BSD-DR-G4,* RAF Institute of Aviation Medicine, Farnborough, Hants, United Kingdom.

Taylor, R.M. (1989). Situational awareness rating technique (SART): The development of a tool for aircrew systems design. In *Proceedings of the AGARD AMP symposium on situational awareness in aerospace operations, CP478,* Seuilly-sur Seine: NATO AGARD.

Taylor, R.M., and Selcon, S.J. (1994). Situation in mind: Theory, applications, and measurement of situational awareness. In R.D. Gilson, D.J. Garland, and J.M. Koonce (Eds.), *Situational Awareness in Complex Systems,* Embry-Riddle Aeronautical University Press.

Warwick, W., McIlwaine, S., Hutton, R., & McDermott, P. (August 2001). Developing computational models of recognition-primed decision making. *Proceedings of the Driving Assessment 2001 Symposium,* 14-17.

Wickens, C.D. (1992). *Engineering psychology and human performance.* New York: Harper-Collins, Inc.

Wickens, C.D., Gordon, S.E., & Liu, Y. (1998). *Introduction to human factors engineering*. New York: Addison Wesley Longman, Inc.

Wickens, C.D., & Hollands, J.G. (2000). *Engineering psychology and human performance*. Upper Saddle River, NJ: Prentice Hall.

Winsum, W.V., & Godthelp, H. (1996). Speed choice and steering behavior in curve driving. *Human Factors, 38*(3), 434-441.

Yardley, L. (1992). Motion sickness and perception: A reappraisal of the sensory conflict approach. *British Journal of Psychology, 83*, 449-471.

Zsambok, C.E., & Klein, G. (1997). *Naturalistic decision making*. Mahwah, NJ: Lawrence Erlbaum and Associates.

NO. OF COPIES ORGANIZATION

1 ADMINISTRATOR
DEFENSE TECHNICAL INFO CTR
ATTN DTIC OCA
8725 JOHN J KINGMAN RD STE 0944
FT BELVOIR VA 22060-6218

1 DIRECTOR
US ARMY RSCH LABORATORY
ATTN AMSRL CI AI R REC MGMT
2800 POWDER MILL RD
ADELPHI MD 20783-1197

1 DIRECTOR
US ARMY RSCH LABORATORY
ATTN AMSRL CI LL TECH LIB
2800 POWDER MILL RD
ADELPHI MD 20783-1197

1 DIRECTOR
US ARMY RSCH LABORATORY
ATTN AMSRL D D SMITH
2800 POWDER MILL RD
ADELPHI MD 20783-1197

1 DIR FOR PERS TECHNOLOGIES
DPY CHIEF OF STAFF PERS
300 ARMY PENTAGON 2C733
WASHINGTON DC 20310-0300

1 OUSD(A)/DDDR&E(R&A)/E&LS
PENTAGON ROOM 3D129
WASHINGTON DC 20301-3080

1 CODE 1142PS
OFC OF NAVAL RSCH
800 N QUINCY STREET
ARLINGTON VA 22217-5000

1 WALTER REED INST OF RSCH
ATTN SGRD UWI C
COL REDMOND
WASHINGTON DC 20307-5100

1 CDR
US ARMY RSCH INST
ATTN PERI ZT DR E M JOHNSON
5001 EISENHOWER AVENUE
ALEXANDRIA VA 22333-5600

NO. OF COPIES ORGANIZATION

1 DEF LOGISTICS STUDIES
INFORMATION EXCHANGE
ATTN DIR DLSIE ATSZ DL
BLDG 12500
2401 QUARTERS ROAD
FORT LEE VA 23801-1705

1 HEADQUARTERS USATRADOC
ATTN ATCD SP
FORT MONROE VA 23651

1 CDR USATRADOC
COMMAND SAFETY OFC
ATTN ATOS MR PESSAGNO/MR LYNE
FORT MONROE VA 23651-5000

1 DIRECTOR TDAD DCST
ATTN ATTG C
BLDG 161
FORT MONROE VA 23651-5000

1 HQ USAMRDC
ATTN SGRD PLC
FORT DETRICK MD 21701

1 CDR
USA AEROMEDICAL RSCH LAB
ATTN LIBRARY
FORT RUCKER AL 36362-5292

1 US ARMY SAFETY CTR
ATTN CSSC SE
FORT RUCKER AL 36362

1 CHIEFARMY RSCH INST
AVIATION R&D ACTIVITY
ATTN PERI IR
FORT RUCKER AL 36362-5354

1 AF FLIGHT DYNAMICS LAB
ATTN AFWAL/FIES/SURVIAC
WRIGHT PATTERSON AFB OH
45433

1 US ARMY NATICK RD&E CTR
ATTN STRNC YBA
NATICK MA 01760-5020

1 US ARMY TROOP SUPPORT CMD
NATICK RD&E CTR
ATTN BEHAVIORAL SCI DIV SSD
NATICK MA 01760-5020

NO. OF COPIES ORGANIZATION

1 US ARMY TROOP SUPPORT CMD
NATICK RD&E CTR
ATTN TECH LIB (STRNC MIL)
NATICK MA 01760-5040

1 DR RICHARD JOHNSON
HEALTH & PERFORMANCE DIV
US ARIEM
NATICK MA 01760-5007

1 NAVAL SUB MED RSCH LAB
MEDICAL LIB BLDG 148
BOX 900 SUBMARINE BASE
NEW LONDON
GROTON CT 06340

1 USAF ARMSTRONG LAB/CFTO
ATTN DR F W BAUMGARDNER
SUSTAINED OPERATIONS BR
BROOKS AFB TX 78235-5000

1 CDR
USAMC LOGISTICS SUP ACTIVITY
ATTN AMXLS AE
REDSTONE ARSENAL AL
35898-7466

1 ARI FIELD UNIT FT KNOX
BLDG 2423 PERI IK
FORT KNOX KY 40121-5620

1 CDR
WHITE SANDS MISSILE RANGE
ATTN STEWS TE RE
WSMR NM 88002

1 STRICOM
12350 RSCH PARKWAY
ORLANDO FL 32826-3276

1 CDR
USA COLD REGIONS TEST CTR
ATTN STECR TS A
APO AP 96508-7850

1 GOVT PUBLICATIONS LIB
409 WILSON M
UNIVERSITY OF MINNESOTA
MINNEAPOLIS MN 55455

NO. OF COPIES ORGANIZATION

1 DR RICHARD PEW
BBN SYSTEMS &TECH CORP
10 MOULTON STREET
CAMBRIDGE MA 02138

1 DR ANTHONY DEBONS
IDIS UNIV OF PITTSBURGH
PITTSBURGH PA 15260

1 MR R BEGGS
BOEING-HELICOPTER CO
P30-18
PO BOX 16858
PHILADELPHIA PA 19142

1 DR ROBERT KENNEDY
ESSEX CORPORATION STE 227
1040 WOODCOCK ROAD
ORLANDO FL 32803

1 LAWRENCE C PERLMUTER PHD
UNIV OF HEALTH SCIENCES
THE CHICAGO MEDICAL SCHOOL
DEPT OF PSYCHOLOGY
3333 GREEN BAY ROAD
NORTH CHICAGO IL 60064

1 GENERAL DYNAMICS
LAND SYSTEMS DIV LIBRARY
PO BOX 1901
WARREN MI 48090

1 GMC N AMER OPERATIONS
PORTFOLIO ENGINEERING CTR
HUMAN FACTORS ENGINEERING
ATTN A J ARNOLD STAFF
PROJ ENG
ENGINEERING BLDG
30200 MOUND RD BOX 9010
WARREN MI 48090-9010

1 DR MM AYOUB DIRECTOR
INST FOR ERGONOMICS RSCH
TEXAS TECH UNIVERSITY
LUBBOCK TX 79409

1 DELCO DEF SYS OPERATIONS
ATTN RACHEL GONZALES B204
7410 HOLLISTER AVE
GOLETA CA 93117-2583

NO. OF COPIES ORGANIZATION

1 MR WALT TRUSZKOWSKI
NASA/GODDARD SPACE
FLIGHT CTR
CODE 588.0
GREENBELT MD 20771

1 US ARMY
ATTN AVA GEDDES
MS YA:219-1
MOFFETT FIELD CA 94035-1000

1 CDR US ARMY RSCH INST OF
ENVIRONMNTL MEDICINE
NATICK MA 01760-5007

1 HQDA (DAPE ZXO)
ATTN DR FISCHL
WASHINGTON DC 20310-0300

1 HUMAN FACTORS ENG PROGRAM
DEPT OF BIOMEDICAL ENGNG
COLLEGE OF ENGINEERING &
COMPUTER SCIENCE
WRIGHT STATE UNIVERSITY
DAYTON OH 45435

1 CDR
USA MEDICAL R&D COMMAND
ATTN SGRD PLC LTC K FRIEDL
FT DETRICK MD 21701-5012

1 PEO ARMORED SYS MODERNIZATION
US ARMY TANK-AUTOMOTIVE CMD
ATTN SFAE ASM S
WARREN MI 48397-5000

1 PEO COMMUNICATIONS
ATTN SFAE CM RE
FT MONMOUTH NJ 07703-5000

1 PEO AIR DEF
ATTN SFAE AD S
US ARMY MISSILE COMMAND
REDSTONE ARSENAL AL
35898-5750

1 PEO STRATEGIC DEF
PO BOX 15280 ATTN DASD ZA
US ARMY STRATEGIC DEF CMD
ARLINGTON VA 22215-0280

NO. OF COPIES ORGANIZATION

1 PROGRAM MANAGER RAH-66
ATTN SFAE AV RAH
BLDG 5681 WOOD RD
REDSTONE ARSENAL AL 35898

1 JON TATRO
HUMAN FACTORS SYS DESIGN
BELL HELICOPTER TEXTRON INC
PO BOX 482 MAIL STOP 6
FT WORTH TX 76101

1 CHIEF CREW SYS INTEGRATION
SIKORSKY AIRCRAFT M/S S3258
NORTH MAIN STREET
STRATFORD CT 06602

1 GENERAL ELECTRIC COMPANY
ARMAMENT SYS DEPT RM 1309
ATTN HF/MANPRINT R C MCLANE
LAKESIDE AVENUE
BURLINGTON VT 05401-4985

1 JOHN B SHAFER
250 MAIN STREET
OWEGO NY 13827

1 OASD (FM&P)
WASHINGTON DC 20301-4000

1 COMMANDANT
US ARMY ARMOR SCHOOL
ATTN ATSB CDS
FT KNOX KY 40121-5215

1 CDR
US ARMY AVIATION CTR
ATTN ATZQ CDM S
FT RUCKER AL 36362-5163

1 CDR
US ARMY SIGNAL CTR &
FT GORDON
ATTN ATZH CDM
FT GORDON GA 30905-5090

1 DIRECTOR
US ARMY AEROFLIGHT
DYNAMICS DIR
MAIL STOP 239-9
NASA AMES RSCH CTR
MOFFETT FIELD CA 94035-1000

NO. OF
COPIES ORGANIZATION

1 CDR
MARINE CORPS SYSTEMS CMD
ATTN CBGT
QUANTICO VA 22134-5080

1 DIR AMC-FIELD ASSIST IN
SCIENCE & TECHNOLOGY
ATTN AMC-FAST
FT BELVOIR VA 22060-5606

1 CDR
US ARMY FORCES CMD
ATTN FCDJ SA BLDG 600
AMC FAST SCIENCE ADVISER
FT MCPHERSON GA 30330-6000

1 CDR
I CORPS AND FORT LEWIS
AMC FAST SCIENCE ADVISER
ATTN AFZH CSS
FORT LEWIS WA 98433-5000

1 HQ III CORPS & FORT HOOD
OFC OF THE SCIENCE ADVISER
ATTN AFZF CS SA
FORT HOOD TX 76544-5056

1 CDR
HQ XVIII ABN CORPS & FT BRAGG
OFC OF THE SCI ADV BLDG 1-1621
ATTN AFZA GD FAST
FORT BRAGG NC 28307-5000

1 SOUTHCOM WASHINGTON
FIELD OFC
1919 SOUTH EADS ST STE L09
AMC FAST SCIENCE ADVISER
ARLINGTON VA 22202

1 HQ US SPECIAL OPERATIONS CMD
AMC FAST SCIENCE ADVISER
ATTN SOSD
MACDILL AIR FORCE BASE
TAMPA FL 33608-0442

1 HQ US ARMY EUROPE AND
7TH ARMY
ATTN AEAGX SA
OFC OF THE SCIENCE ADVISER
APO AE 09014

NO. OF
COPIES ORGANIZATION

1 CDR
HQ 21ST THEATER ARMY AREA CMD
AMC FAST SCIENCE ADVISER
ATTN AERSA
APO AE 09263

1 HQ 7TH ARMY TRAINING CMD
UNIT #28130
AMC FAST SCIENCE ADVISER
ATTN AETT SA
APO AE 09114

1 CDR HHC SOUTHERN EUROPEAN
TASK FORCE
ATTN AESE SA BLDG 98
AMC FAST SCIENCE ADVISER
APO AE 09630

1 CDR US ARMY PACIFIC
AMC FAST SCIENCE ADVISER
ATTN APSA
FT SHAFTER HI 96858-5L00

1 AMC FAST SCIENCE ADVISERS
PCS #303 BOX 45 CS-SO
APO AP 96204-0045

1 ENGINEERING PSYCH LAB
DEPT OF BEHAVIORAL
SCIENCES & LEADERSHIP
BLDG 601 ROOM 281
US MILITARY ACADEMY
WEST POINT NY 10996-1784

3 DIR SANDIA NATL LAB
ENGNRNG MECHANICS DEPT
MS 9042 ATTN J HANDROCK
Y R KAN J LAUFFER
PO BOX 969
LIVERMORE CA 94551-0969

1 DR SEHCHANG HAH
WM J HUGHES TECH CTR FAA
NAS HUMAN FACTORS BR
ACT-530 BLDG 28
ATLANTIC CITY INTNATL
AIRPORT NJ 08405

1 US ARMY RSCH INST
ATTN PERI IK D L FINLEY
2423 MORANDE STREET
FORT KNOX KY 40121-5620

NO. OF COPIES ORGANIZATION

1 US MILITARY ACADEMY
MATHEMATICAL SCIENCES CTR
OF EXCELLENCE
DEPT OF MATH SCIENCES
ATTN MDN A MAJ HUBER
THAYER HALL
WEST POINT NY 10996-1786

1 NAIC/DXLA
4180 WATSON WAY
WRIGHT PATTERSON AFB OH
45433-5648

1 CDR USA TACOM
ATTN TECH LIBRARY
WARREN MI 48397

1 CDR US ARMY ARMOR SCHOOL
ATTN TECH LIBRARY
FT KNOX KY 40121

5 CDR USA TACOM
ATTN AMSTA TR R (MS264 BRENDLE)
WARREN MI 48397-5000

1 CPT ANGUS RUPERT
MC US NAVY
51 HOVEY RD
PENSACOLA FL 32508-1046

1 RSK ASSESSMENTS INC
ATTN ROBERT KENNEDY
1040 WOODCOCK RD STE 227
ORLANDO FL 32803

1 ARL HRED AVNC FLD ELMT
ATTN AMSRL HR MJ D DURBIN
BLDG 4506 (DCD) RM 107
FT RUCKER AL 36362-5000

1 ARL HRED AMCOM FLD ELMT
ATTN AMSRL HR MI
BLDG 5464 RM 202
REDSTONE ARSENAL AL
35898-5000

1 ARL HRED AMCOM FLD ELMT
ATTN AMSRL HR MO T COOK
BLDG 5400 RM C242
REDSTONE ARS AL 35898-7290

NO. OF COPIES ORGANIZATION

1 ARL HRED USAADASCH FLD ELMT
ATTN AMSRL HR ME K REYNOLDS
ATTN ATSA CD
5800 CARTER ROAD
FORT BLISS TX 79916-3802

1 ARL HRED ARDEC FLD ELMT
ATTN AMSRL HR MG R SPINE
BUILDING 333
PICATINNY ARSENAL NJ
07806-5000

1 ARL HRED ARMC FLD ELMT
ATTN AMSRL HR MH C BURNS
BLDG 1002 ROOM 206B
1ST CAVALRY REGIMENT RD
FT KNOX KY 40121

1 ARL HRED CECOM FLD ELMT
ATTN AMSRL HR ML J MARTIN
MYER CENTER RM 2D311
FT MONMOUTH NJ 07703-5630

1 ARL HRED FT BELVOIR FLD ELMT
ATTN AMSRL HR MK
10170 BEACH RD
FORT BELVOIR VA 22060-5800

1 ARL HRED FT HOOD FLD ELMT
ATTN AMSRL HR MV HQ USAOTC
S MIDDLEBROOKS
91012 STATION AVE ROOM 111
FT HOOD TX 76544-5073

1 ARL HRED FT HUACHUCA
FIELD ELEMENT
ATTN AMSRL HR MY M BARNES
RILEY BARRACKS BLDG 51005
FT HUACHUCA AZ 85613

1 ARL HRED FLW FLD ELMT
ATTN AMSRL HR MZ A DAVISON
320 MANSCEN LOOP STE 166
FT LEONARD WOOD MO 65473-8929

1 ARL HRED NATICK FLD ELMT
ATTN AMSRL HR MQ M FLETCHER
NATICK SOLDIER CTR BLDG 3
RM 341 AMSSB RSS E
NATICK MA 01760-5020

NO. OF
COPIES ORGANIZATION

1 ARL HRED OPTEC FLD ELMT
ATTN AMSRL HR MR H DENNY
ATEC CSTE PM ARL
4501 FORD AVE RM 870
ALEXANDRIA VA 22302-1458

1 ARL HRED SC&FG FLD ELMT
ATTN AMSRL HR MS R ANDERS
SIGNAL TOWERS RM 303A
FORT GORDON GA 30905-5233

1 ARL HRED STRICOM FLD ELMT
ATTN AMSRL HR MT A GALBAVY
12350 RESEARCH PARKWAY
ORLANDO FL 32826-3276

1 ARL HRED TACOM FLD ELMT
ATTN AMSRL HR MU M SINGAPORE
6501 E 11 MILE RD MAIL STOP 284
BLDG 200A 2ND FL RM 2104
WARREN MI 48397-5000

1 ARL HRED USAFAS FLD ELMT
ATTN AMSRL HR MF L PIERCE
BLDG 3040 RM 220
FORT SILL OK 73503-5600

1 ARL HRED USAIC FLD ELMT
ATTN AMSRL HR MW E REDDEN
BLDG 4 ROOM 332
FT BENNING GA 31905-5400

1 ARL HRED USASOC FLD ELMT
ATTN AMSRL HR MN R SPENCER
DCSFDI HF
HQ USASOC BLDG E2929
FORT BRAGG NC 28310-5000

1 ARL HRED HFID FLD ELMT
ATTN AMSRL HR MP
D UNGVARSKY
BATTLE CMD BATTLE LAB
415 SHERMAN AVE UNIT 3
FT LEAVENWORTH KS 66027-2326

1 CDR AMC - FAST
JRTC & FORT POLK
ATTN AFZX GT DR J AINSWORTH
CMD SCIENCE ADVISOR G3
FORT POLK LA 71459-5355

NO. OF
COPIES ORGANIZATION

1 CDR HRED AMEDD
ATTN AMSRL HR MM COL N VAUSE
2250 STANLEY RD STE 322
FT SAM HOUSTON TX 78234

ABERDEEN PROVING GROUND

2 DIRECTOR
US ARMY RSCH LABORATORY
ATTN AMSRL CI LP (TECH LIB)
BLDG 305 APG AA

1 LIBRARY
ARL BLDG 459
APG-AA

1 ARL HRED
ATTN AMSRL HR MB
F PARAGALLO
BLDG 459

1 US ATEC
RYAN BLDG
APG-AA

REPORT DOCUMENTATION PAGE

Form Approved
OMB No. 0704-0188

1. AGENCY USE ONLY *(Leave blank)*	2. REPORT DATE	3. REPORT TYPE AND DATES COVERED
	May 2002	Final

4. TITLE AND SUBTITLE

Modeling Indirect Vision Driving With Fixed Flat Panel Displays: Task Performance and Mental Workload

5. FUNDING NUMBERS

AMS Code 622716
PR: AH70

6. AUTHOR(S)

Smyth, C.C. (ARL)

7. PERFORMING ORGANIZATION NAME(S) AND ADDRESS(ES)

U.S. Army Research Laboratory
Human Research & Engineering Directorate
Aberdeen Proving Ground, MD 21005-5425

8. PERFORMING ORGANIZATION REPORT NUMBER

9. SPONSORING/MONITORING AGENCY NAME(S) AND ADDRESS(ES)

U.S. Army Research Laboratory
Human Research & Engineering Directorate
Aberdeen Proving Ground, MD 21005-5425

10. SPONSORING/MONITORING AGENCY REPORT NUMBER

ARL-TR-2701

11. SUPPLEMENTARY NOTES

12a. DISTRIBUTION/AVAILABILITY STATEMENT

Approved for public release; distribution is unlimited.

12b. DISTRIBUTION CODE

13. ABSTRACT *(Maximum 200 words)*

The relation between mental workload and situational awareness and the effects on vehicle performance are of interest to designers of future combat ground vehicles. In this report, a micro-state task time line analysis of attention workload is used to describe a model of driving performance and mental workload for indirect vision driving. The model is based on the results of a field study in which a military vehicle was driven with flat panel, liquid crystal displays fixed in the cab and a forward viewing monocular camera array mounted on the front roof. The task load times for the model are calculated with a mathematical equation for vehicle speed as a function of the camera field of view. The vehicle speed equation is derived with consideration given to the effects of scene compression on the informational needs of the driver in a self-paced task. An analysis shows that the task performance and mental workload are separable for the short course runs used in the field study. The effect of indirect vision driving on mental workload is determined from the subjective ratings of perceived task loading that were reported in the field study. Along with the perceived workload, the study participants rated the mental measures of task allocated attention, situational awareness, motion sickness, and subjective stress. Because of collinearity, the perceived workload is regressed on the factorial components of a cognitive loading space derived from a factorial analysis of the mental measures. Following rotation to a "skills-rules-knowledge" cognitive processing space derived from the clustering of the measures, the perceived workload is shown to be a function of the skills and rule-based components. On this basis, a micro-state time line model is proposed for the task information processing. In addition to the attention allocated to the driving task, the model includes attention to cognitive maps for route navigation and the monitoring of the internal somatic state for motion sickness. The task loading measures generated by the model are compared to the reported values with significant results. Finally, the model results are used to construct information flow networks for task analysis workload simulation studies. The model is intended for future work in predicting fatigue and performance errors that are induced by mental workload during indirect vision driving.

14. SUBJECT TERMS

driving
indirect vision driving
mental workload
motion sickness

15. NUMBER OF PAGES
85

16. PRICE CODE

17. SECURITY CLASSIFICATION OF REPORT	18. SECURITY CLASSIFICATION OF THIS PAGE	19. SECURITY CLASSIFICATION OF ABSTRACT	20. LIMITATION OF ABSTRACT
Unclassified	Unclassified	Unclassified	